AWARD NUMBER: W81XWH-15-1-0607

TITLE: The Effect of the Elimination of Micromotion and Tissue Strain on Intracortical Device Performance

PRINCIPAL INVESTIGATOR: Joseph J. Pancrazio

CONTRACTING ORGANIZATION: The University of Texas at Dallas
Richardson, TX 75080

REPORT DATE: October 2016

TYPE OF REPORT: Annual

PREPARED FOR: U.S. Army Medical Research and Materiel Command
Fort Detrick, Maryland 21702-5012

REPORT DOCUMENTATION PAGE

Form Approved
OMB No. 0704-0188

1. REPORT DATE	2. REPORT TYPE	3. DATES COVERED
October 2016	Annual	30 Sep 2015 –29 Sep 2016

4. TITLE AND SUBTITLE

The Effect of the Elimination of Micromotion and Tissue Strain on Intracortical Device Performance

5a. CONTRACT NUMBER

5b. GRANT NUMBER
W81XWH-15-1-0607

5c. PROGRAM ELEMENT NUMBER

6. AUTHOR(S)
Joseph J. Pancrazio

E-Mail: jjp150430@utdallas.edu

5d. PROJECT NUMBER

5e. TASK NUMBER

5f. WORK UNIT NUMBER

7. PERFORMING ORGANIZATION NAME(S) AND ADDRESS(ES)
University of Texas at Dallas
800 W Campbell Rd
Richardson, TX 75080-1407

8. PERFORMING ORGANIZATION REPORT NUMBER

9. SPONSORING / MONITORING AGENCY NAME(S) AND ADDRESS(ES)

U.S. Army Medical Research and Materiel Command
Fort Detrick, Maryland 21702-5012

10. SPONSOR/MONITOR'S ACRONYM(S)

11. SPONSOR/MONITOR'S REPORT NUMBER(S)

12. DISTRIBUTION / AVAILABILITY STATEMENT

Approved for Public Release; Distribution Unlimited

13. SUPPLEMENTARY NOTES

14. ABSTRACT
Intracortical probes can be used to record brain signals to control paralyzed or robotic prosthetic limbs. Unfortunately, this technology is not reliable, likely for the reason that these devices are made of extremely stiff materials – 1 million times stiffer than the surrounding brain tissue. This difference in stiffness is believed to create inflammation which degrades the brain tissue and leads to device failure. While it has been previously proposed that flexible intracortical probes would exhibit an improved tissue response and enhanced device performance, there have been no definitive studies that definitively test this hypothesis. We are developing intracortical probes using shape memory polymers (SMPs): materials which have the capacity to transition from stiff to soft upon implantation. We will tune the degree of stiffness such that we can definitively address a fundamental question which limits progress in the field: Does probe softening improve the surrounding tissue response and recording performance of the device? The short term impact will be on the scientific community through publications and presentations. Over the long term, the core technology has exceptional promise for translation into the clinic. SMP-based probes are compatible with reliable manufacturing practices.

15. SUBJECT TERMS
Intracortical probe, neuroprosthesis, polymers, neural recording

16. SECURITY CLASSIFICATION OF:			17. LIMITATION OF ABSTRACT	18. NUMBER OF PAGES	19a. NAME OF RESPONSIBLE PERSON
a. REPORT	b. ABSTRACT	c. THIS PAGE			USAMRMC
Unclassified	Unclassified	Unclassified	Unclassified	30	19b. TELEPHONE NUMBER *(include area code)*

Table of Contents

INTRODUCTION

The goal of this research has focused on understanding how a key material property, stiffness, influences the robustness of implantable neuroprosthetic technologies. By bypassing damaged regions of the nervous system, brain machine interfaces (BMIs) offer the promise of reducing the burden of injury, a burden disproportionately borne by veterans, and enabling these injured individuals to live more full and interactive lives. Unfortunately, these devices, which take the form of implantable microelectrode arrays or intracortical probes, do not demonstrate long-term robustness. A major aspect of this issue has been hypothesized to be due to the differential stiffness between the implantable device and surrounding brain tissue. We are leveraging state-of-the-art shape memory polymer (SMP) material science where the degree of material softening can be precisely controlled in order to systematically address the importance of implantable device softening in the brain for robust intracortical probe performance. In addition, the fabrication approaches used to create these test structures take advantage of industrial level manufacturing processes such that promising technology arising from this proposal has the capacity for translation by leveraging standard semiconductor processing techniques.

KEYWORDS

cyclic voltammetry, cytotoxicity, dynamic mechanical analysis, electrochemical impedance spectroscopy, immunohistochemistry, micromotion, modulus, shape memory polymer, sterilization, insulation

ACOMPLISHMENTS

The table below lists the specific aims as proposed and the status of the subtasks as identified in the SOW. This report covers the performance relative to Lead Investigators Dr. Pancrazio and Dr. Voit of the University of Texas at Dallas (Site 1) (for review of progress from Site 2, please refer to the companion report from Dr. Capadona from Cleveland VA which is Site 2 below). Based on the timeline, the subtasks that are relevant to this 1st year report from Dr. Pancrazio and Voit are highlighted below.

Specific Aim (as specified in proposal)	**Timeline**	**Site 1**	**Site 2**	**Status**
Specific Aim 1: Quantitatively compare the tissue response evoked by short term and chronic implantation of non-softening, moderately softening, and softening shape memory polymer (SMP)-based intracortical probes.	**Months**	**Lead Investigator(s)**	**Lead Investigator**	**% complete**
Subtask 1: Fabricate non-functional SMP probes and verify physical and thermo-mechanical properties	1-6	Dr. Voit		100%
Subtask 2: Implant all variants of non-functional SMP probes into motor cortex of rats (165 total)	6-18		Dr. Capadona	
Subtask 3: Harvest tissue from non-functional SMP probes implanted rat motor cortex	12-24		Dr. Capadona	
Subtask 4: Comprehensive immunohistochemical analysis of tissue response for acute and chronic SMP-based intracortical probes	18-30		Dr. Capadona	

Subtask 5: Dissemination of data through publication and presentation	24-36	Drs. Pancrazio & Voit	Dr. Capadona	
Milestone Achieved: Identification of distinctive tissue profiles due to differential modulus of non-functional SMP probes		Drs. Pancrazio & Voit	Dr. Capadona	
Milestone Achieved: Local IRB/IACUC approval	3		Dr. Capadona	
Milestone Achieved: HRPO/ACURO approval	6		Dr. Capadona	
Specific Aim 2: Quantitatively compare the long term recording capability of softening and non-softening SMP-based intracortical probes				
Subtask 1: Fabricate functional SMP probes and verify physical and thermo-mechanical properties	1-9	Dr. Voit		70%
Subtask 2: Implant all variants of functional SMP probes into motor cortex of rats (80 total)	6-30	Dr. Pancrazio		0%
Subtask 3: Perform bi-weekly recordings of single unit activity and electrochemical impedance spectroscopy using functional SMP probes	6-33	Dr. Pancrazio		0%
Subtask 4: Equivalent circuit modeling from EIS	27-36	Dr. Pancrazio		
Subtask 5: Comprehensive immunohistochemical analysis of tissue response for chronic SMP-based intracortical probes at identical time to non-functional, and at failure.	24-36	Dr. Pancrazio	Dr. Capadona	
Subtask 6: Dissemination of data through publication and presentation	24-36	Drs. Pancrazio & Voit	Dr. Capadona	
Milestone Achieved: Determination of differential device performance as a function of the modulus of SMP probes	30	Drs. Pancrazio & Voit	Dr. Capadona	
Milestone Achieved: Local IRB/IACUC approval	3	Dr. Pancrazio		100%
Milestone Achieved: HRPO/ACURO approval	6	Dr. Pancrazio		100%

Milestones: Two milestones have been completed during this first reporting period. Specific aim 2 requires the utilization of animal models, of which we selected Long Evans rats which have been used for neurobiological motor research, we needed both our local IACUC and ACURO approval to proceed. The University of Texas at Dallas office of compliance awarded the approval for our protocol for the chronic implantation of the SMP and control Neuronexus probes into the motor cortex on 17 Dec 2016. ACURO approval of this protocol was obtained on 2 Feb 2016. With the approvals, both milestones are 100% and within the specified time limits outlined in the SOW.

Specific Aim 1, Subtask 1 Progress: To complete this subtask, we worked to reproducibly fabricate non-functional intracortical probes consisting of multiple shape memory polymer formulations. The goal was to create and deliver to Site 2 for implantation studies four classes of SMP devices: fully softening; moderately softening; non-softening; and silicon shanks that were thinly coated with softening SMP as a control. Each of these classes consisted of a single shank approximately 30 microns thick, without electrical contacts or connections, but with consistent shape and dimensions (**Figure 1**). In brief, the entire subtask has been fully completed. These non-functional structures were dedicated for implantation in rat motor cortex (at Site 2) to test the idea that those devices that soften the most will demonstrate the least neuroinflammatory response based on immunohistochemical analysis of the tissue. Since we are aiming to ultimately create multi-microelectrode implantable devices comparable to the commercially available Neuronexus (NNx) probe, the planned feature sizes would necessitate the incorporation of 1 μm feature

photolithographic techniques, opposed to laser machining.

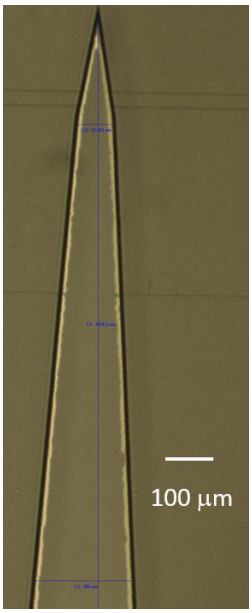

Figure 1: Non-functional intracortical probe fabricated from shape memory polymer.

Controlled and repeatable thicknesses control of the SMP layers was also another very important processing constraint. The generation of spin-coated polymers replaced the previous casting protocols, and we verified the new formulations through the characterization of the thermo-mechanical properties of copolymer films. To create the structures, we adjusted ratios of the thiol-ene and thiol-ene/acrylate formulations: non-softening SMP composed of TMTMP, TATATO, and TCMDA ratios of 0.345, 0.345, and 0.31 (SMP 8); a 10x softening SMP composed of TATATO and TMICN at at 0.5-0.5 ratio (SMP 5), and the 100x softening SMP formulations of TMTMP and TATATO at the 0.5, 0.5 ratio (SMP 7). Briefly, the fabrication of the SMP polymer films involves combining the monomers, spin coating the combined polymer solution on a glass substrate, and photo-curing at a wavelength of 254 nm for 2 hours. Post-curing is performed in an oven under vacuum at 120 °C. **Figure 1** shows a fabricated non-functional probe, in this instance created from formulations that allow the structure to entirely soften after implantation.

To verify that a particular SMP sample or device has the desired thermo-mechanical properties, dynamic mechanical analysis (DMA) is performed to extract parameters including: the glass transition temperature (T_g), glassy modulus, rubbery modulus, and tangent delta. Previously our tests of these parameters were based on dry measurements with projection of the expected behavior under aqueous conditions. *We have substantially improved our characterization of the properties by making use of a new aqueous phase, temperature controlled DMA system that accommodates immersed samples with an environmental chamber.* Our DMA immersion system allowed us to mimic *in vivo* conditions relevant for implantable devices. We verified that the polymers were able to undergo various degrees of softening at physiological conditions, meeting the 100x softening, 10x softening and non-softening requirements for the project (**Figure 2**).

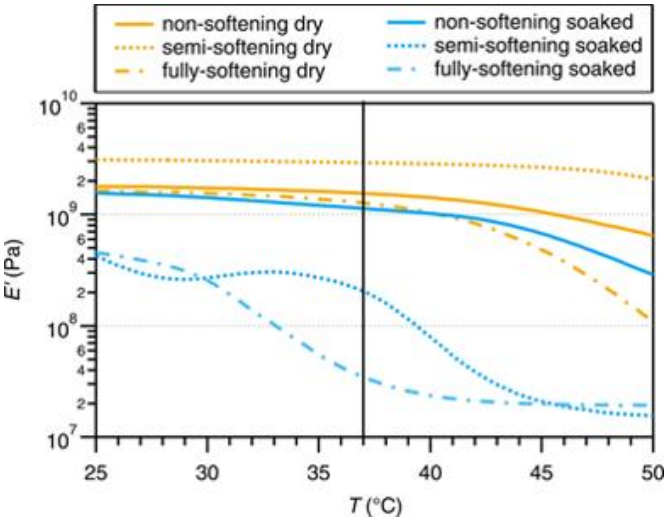

Figure 2: Dynamic Mechanical Analysis of the three SMP compositions displaying modulus as a function of temperature change. Orange shows the modulus (E') for the polymers when measured in a dry air environment and blue shows the polymers when immersed in phosphate buffered saline.

There is a well-established literature on the histological profile induced by chronic implantation of stiff implanted intracortical probes. However, it has been reported that incomplete sterilization of these test devices can produce infections that manifest inflammation and confound the interpretation of the data[1]. For SMP based bioelectronic applications, the question of

[1] Ravikumar et al. (2014) "The Effect of Residual Endotoxin Contamination on the Neuroinflammatory Response to Sterilized Intracortical Microelectrodes" J Mater Chem B Mater Biol Med. 2(17): 2517–2529. doi: 10.1039/C3TB21453B.

whether or not these unique materials can tolerate sterilization procedures has been a standing question. In fact, for our studies, it is imperative that sterilization either not alter the softening capability or at least we need to be able to design for any shift in thermo-mechanical properties. Therefore, for all the formulations of SMP devices, we examined the non-functional test device robustness and mechanical properties with different sterilization procedures. It is also important to recognize that eventual translation from the laboratory to clinical use requires that medical devices can tolerate sterilization. Established methods, accepted by the Food and Drug Administration, include steam, ethylene oxide (EtO), and ultraviolet radiation. We have recently published an article (Ecker et al., 2016) detailing a study in which SMP materials were submitted to the aforementioned tests, and the full document is included in the appendix section, pages 21-30. In brief, we have established that devices which use any the fully and non-softening SMP formulations can be effectively sterilized using low temperature EtO exposure, with the materials experiencing no noticeable changes in the modulus profile. We also determined the following SMP deposition and curing via UV exposure, a small heterogeneous surface layer forms that is negligible for bulk samples but has the potential to affect thermo-mechanical properties for thin samples. We showed that with an additional etch step, this heterogeneous layer is removed and consistency is achieved. EtO has also been shown to be safe for electronic components, like electrical (Omnetics) connectors, which was important as we needed not only to create a device with a material that softens in the brain, but also package this device so it can be interfaced with neural recording amplifiers, electrochemical workstations, and associated data acquisition systems.

Specific Aim 2, Subtask 1 Progress: As we had stated in our proposal, our SMP devices have a similar architecture to the NeuroNexus (NNx) commercial A1x16 implants, which also serve as hard material devices for comparison purposes. Additionally, we could also use the same electrical connector, the 18 pin Omnetics connector, with which to connect the implant with the various external testing systems. Over this past year, we have been refining the fabrication processes to ensure reproducible physical and electrical features for devices fabricated from any of the SMP based devices. With well-deposited and distinct microelectrode sites and traces, both consisting of Au, the bigger issue is having good insulation surrounding these bioelectrical interface sites. Nevertheless, we first attempted first to create a device where the SMP itself served as the insulation. We reasoned that tf this worked and the insulating performance of each of the SMP formulations was similar, then functional devices would be relatively simple in composition with only the SMP and the nm thick deposits of gold to create the microelectrode sites and traces (based on the thinness of the Au, the impact on the overall mechanics of the device after implantation would be expected to be entirely negligible). **Figure 3** shows one of our fabricated 16 microelectrode arrays from SMP. Briefly, the device begins as a 15 μm thick film of the particular SMP. The gold traces and microelectrode pads are formed by sputtering, photolithographic techniques, and a wet etch performed in the UT Dallas Cleanroom. A final layer of SMP is added, the windows for the pads and trace connections are opened using reactive ion etching (RIE) with CF_4O_2 plasma, and a shank and connector tab for the device shape are formed using a RIE step. An 18 pin Omnetics connector is soldered directly onto the surface of the SMP Tab and encapsulated with surgical grade Loctite Hysol Medical grade device epoxy. Our first test devices were composed of SMP 7, the fully softening polymer. Close examination of our initial devices indicated two major issues in our fabrication process. **Figure 3(b)** shows an optical micrograph detailing the surface of the shank. The windows around each of the microelectrode sites had a diameter much larger than the

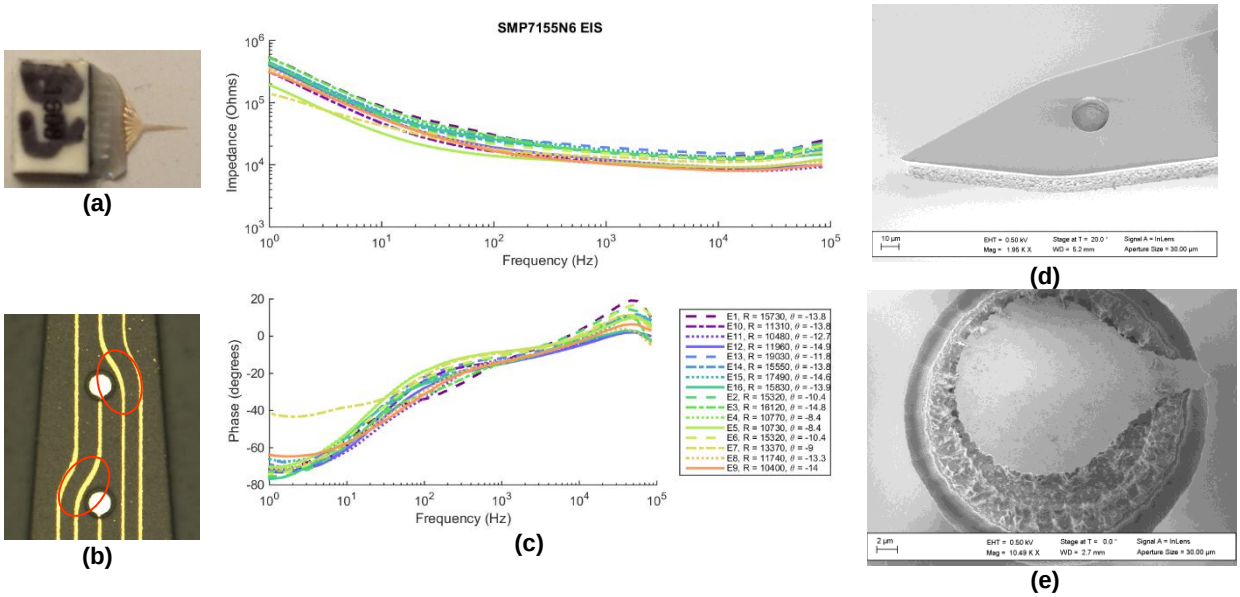

Figure 3: **(a)** one of our initial NNx style SMP 7 (fully-softening) chronic microelectrode probes with gold microelectrodes and traces. **(b)** An optical micrograph of the surface of the shank for one of the SMP7 NNx style devices. The red circles indicate areas locations where the windows for the microelectrode sites display over etching, possibly allowing electrochemical cross-talk between multiple microelectrodes. Also noticed in the image is that the traces show indications of variable width, and gold particles in between traces, both of which can contribute to electrical performance issues. **(c)** Electrochemical impedance spectroscopy (EIS) of all 16 microelectrodes from a representative SMP NNx style probe. The legend displays the impedance for each microelectrode site measured at 1 KHz. **(d)** and **(e)** scanning electron microscope (SEM) micrographs of microelectrode 1 at the tip of the device. The SEM shows the extent of the over etching is not only lateral, but the SMP surface is extremely damaged and there may also be some undercutting of the SMP beneath the metal microelectrode.

original 15 μm design, and appeared large enough to even uncover traces from other microelectrodes.

The SMP7 devices were tested electrochemically with a Model 604E Electrochemical Analyzer/Workstation (CH Instruments, Austin, TX) in phosphate buffered solution (PBS) at 7.4 pH. The results for the electrochemical impedance spectroscopy (EIS) from 100 KHz to 1 Hz, 5 mV_{pp}, 12 points/ decade for one of the 16 microelectrode devices are shown in **Figure 3(c)**. The first impression of these devices is that the impedance is incredibly low for a gold microelectrode with a geometric surface area of 176 μm^2, exhibiting a 10 – 20 KΩ resistance at 1 KHz. The same size microelectrode sites on the NNx devices, which are composed of iridium, have an impedance range of 700 – 900 KΩ at 1 KHz. Although the resistivity of iridium is twice that of gold, and the electrochemical interface creates a more complex impedance model, the large impedance discrepancy most likely indicates that the gold microelectrodes on the initial SMP devices were damaged. Furthermore, extreme surface damage within the etched windows along with additional SMP material under-cutting beneath the electrode edges was observed, as displayed in the SEM micrographs in **Figure 3(d)** and **(e)**. Examination of the fabrication process stages revealed the over etch was due to our etching process in conjunction with our RIE etching parameters.

We first worked to refine the feature sizes of the single microelectrode sites. Conventional polymeric masking does not provide enough mask removal options, so used silicon nitride (Si_3N_4) as the SMP etch mask. After deposition of Si_3N_4 on the SMP, we masked it with Shipley' 1813 photoresist, developed the photoresist, and then etched the Si_3N_4 using CF_4O_2

RIE. The RIE plasma was switched to an O_2 source, which appears to be more effective at etching the SMP polymer formulations. **Figure 4 (a) – (d)** displays the progression of the etch window through the multiple lithography and etch processes, with the radius of the etch window nearly doubling in size after the final etch. **Figure 4(e) and (f)** shows electrodes on the SMP implant which were fabricated with our new improved etching process. Each of the windows consistently measure approximately 15 μm in diameter and no longer exposed any adjacent wire traces. In summary, the etching issues wereresolved through a decrease in pressure from 120 mTorr to 100 mTorr and a switch from CF_4O_2 to SF_6 etching plasma.

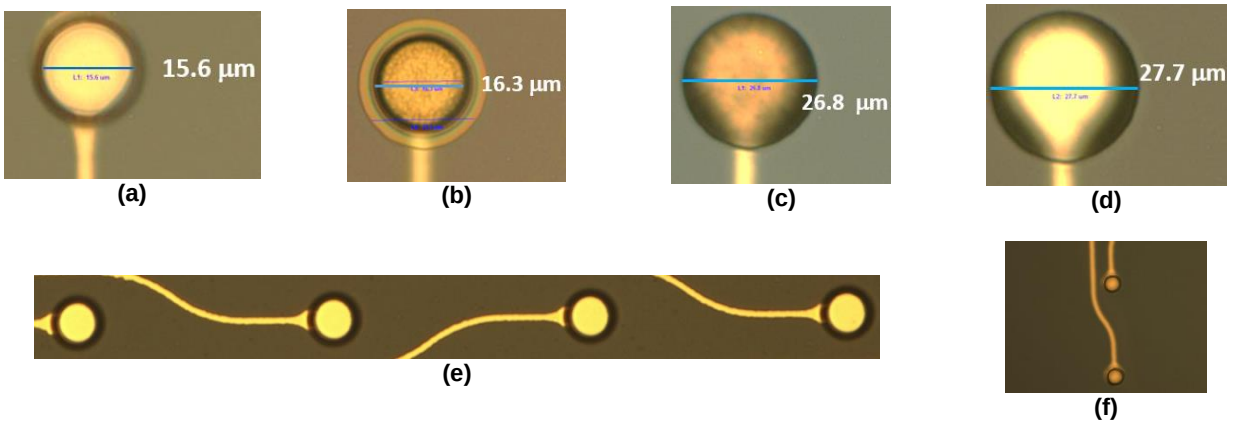

Figure 4: **(a)** through **(d)** are optical micrographs of a single electrode as observed through each stage of etching. **(a)** The Shipley's 1813 photoresist has a 15.6 μm hole after UV exposure and developing. **(b)** The size of the window in the Si_3N_4 mask increased to 16.3 μm diameter after CF_4O_2 RIE, which is an indication of etch mask undercutting. **(c)** After the O_2 plasma etch of the SMP, the window increases to 26.8 μm diameter, and finally 27.7 μm diameter after the Si_3N_4 mask has been removed **(d)**. **(e)** and **(f)** indicate that the newly developed etching process consistently generated electrode windows that are within 10% of the designed size.

We next worked on the problem of gold particulates which we considered to be due to the gold wet etch. The standard approach for etching gold on semiconductor (e.g., silicon) substrates is the TFA gold etch, an iodine ($KI-I_2$) based process. While the SMPs are not explicitly damaged by this etch method, it appears that the anisotropic nature of wet etching, produces variable etching rates across the surface of the gold. Moreover, **Figure 5(a)** and **(b)** show that this etching method leaves gold particulates located in-between the traces of the microelectrodes. These particulates could be removed with additional etching time, but that would inevitably lead to etching beneath the mask layer, producing irregularities in the sidewalls of the traces and pads (**Figure 5(c)**). To address this issue, we exploited another a fabrication process used in semiconductor processing. The liftoff process usually uses a polymer based mask on which a metal is evaporated or sputtered. The polymer is then removed with a solvent like acetone, leaving metal only on the surfaces which the polymer did not cover. As solvents could damage the SMP, we developed a new liftoff process. The liftoff process starts with the initial SMP base layer receiving 500 nm of plasma enhanced chemical vapor deposition (PECVD) parylene-C. Si_3N_4 is deposited next and patterned nLOF 2026 photoresist. In this case, we use the RIE with SF_6 plasma to intentionally slightly undercut the photoresist mask. Ti/ Au/ Ti metal is deposited using electron-beam evaporation with thickness of 25 nm/ 400nm/ 25nm. Hydrofluoric acid in deionized water (1:10 ratio) etches the Si_3N_4 mask, taking the excess metal with it and leaving only metal in the desired locations. **Figure 5(d)** shows that the discrepancy seen with the microelectrode and trace widths and sidewalls have been eliminated with the lift-off process. **Figure 5(e)** shows that the gold particulates lodged between the traces have also been eliminated.

With gold deposition and etching established, we focused on ensuring consistent insulating

behavior surrounding the gold microstructures. Without consistent insulation, interpreting changes in the ability of different SMP devices to record units in vivo would not be possible. Stable recording microelectrodes should have a consistent impedance over time and degradation of insulation quality would emerge as a reduction in impedance.

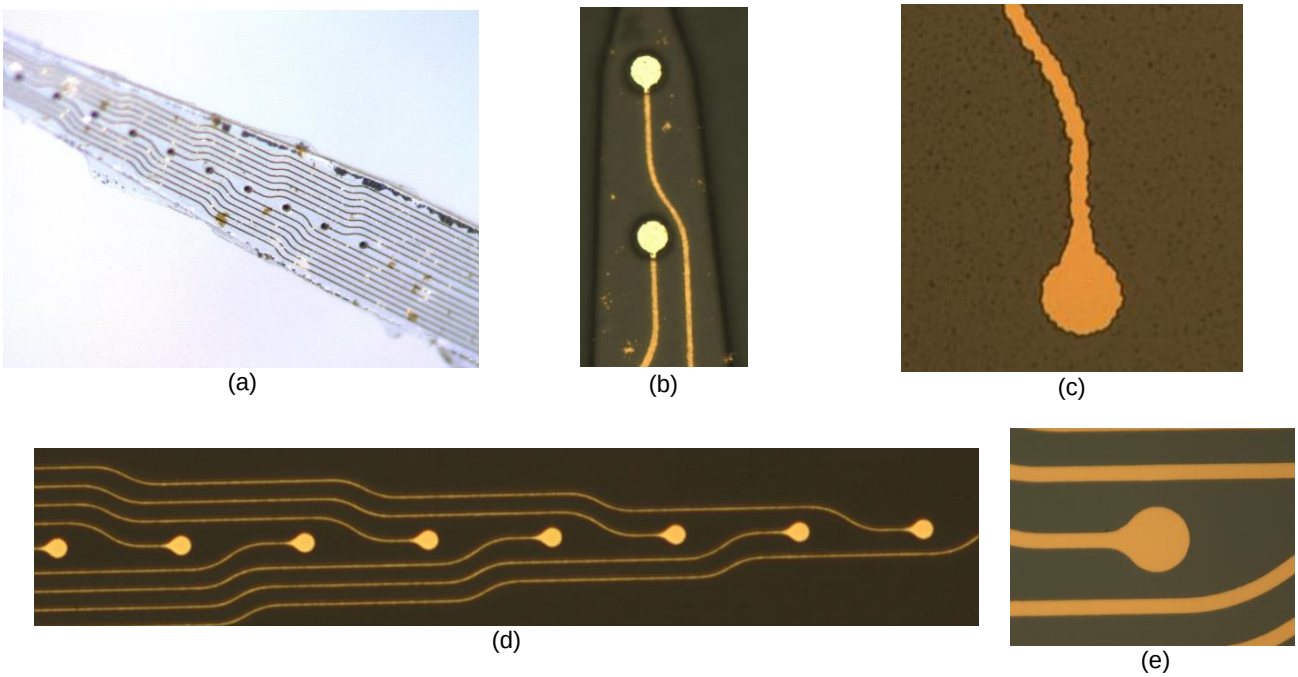

Figure 5: **(a)** An optical micrograph of the shank from a SMP NNx style electrode. Flakes of gold and other particulates are clearly visible within the SMP insulation throughout the device. **(b)** Another optical micrograph showing against a darker background that accentuates the gold particles inside the SMP device. **(c)** An optical micrograph taken after the wet etch of gold showing that additional etching time produced over and irregular etching of the edges of the pads and traces, most likely due to anisotropic etching under the mask. **(d)** and **(e)** Optical micrographs of the gold pads and traces on SMP after the Si_3N_4 liftoff process. The pads and traces are well within tolerances, have well defined edge profiles, and the gold particles embedded in the SMP have been eliminated.

To utilize the full potential of the SMP mechanical properties, the ideal device would not only use SMP as the main structure, but also capitalize on it as polymer insulator; however, the resistivity of the different SMP formulations was unknown. To evaluate the electrical performance of the SMP, we relied on a previously developed testing methodology involving interdigitated electrodes (IDEs)[2], where these test structures were readily fabricated of the main materials of planned for the SMP-based devices. The IDEs are encapsulated within the insulating layers then immersed within 7.4 pH PBS at 37°C and monitored for stability. Three electrochemical tests are then systematically performed on the devices. The first, EIS, is evaluated from 100 KHz to 0.1 Hz at 12 points a decade using a 50 mV_{rms} sinusoidal signal centered at the open circuit potential. The second test is cyclic voltammetry (CV) run from -0.6 V to 0.6 V at a rate of 50 mV/ s and sampled at 0.01 s. The final test uses chronoamperometry (CA) with a 5 VDC square pulse at 50% duty cycle over 300 s. If the insulation fails, the gold microelectrodes will be exposed to the PBS and the impedance will change dramatically. Failure of the device occurs if the real impedance falls below 0.1 GΩ below 1 Hz, if the phase goes more positive than -80 ° above 1 Hz (which signifies a transition from more capacitive to resistive character consistent with leakage paths), or if the

[2] Minnikanti et al. (2013) Lifetime assessment of atomic-layer-deposited Al2O3-Parylene C bilayer coating for neural interfaces using accelerated age testing and electrochemical characterization. Acta Biomater. 10(2):960-7. doi: 10.1016/j.actbio.2013.10.031

leakage current goes above 1 nA for the CA and CV tests. Three IDE structures were fabricated using the different SMP formulations as insulators. Each of the structures consisted of two working electrodes, located on the outside edges, and a single common common/ reference electrode down the center of the device. The electrodes were encapsulated in 15 μm of SMP on each side. An optical micrograph of a fabricated SMP IDE structure is shown in **Figure 6(a)**. Representative graphs impedance obtained from the long term *in vitro* test is shown in **Figure 6(b)** for the non- (SMP 8) and fully-softening (SMP 7) IDE electrodes. What was discovered in the test is that the SMP 7 and SMP 5 (semi-softening) devices fell below acceptable levels at day 7 and 12 days, respectively. SMP 8 was able to maintain the high impedance necessary for an appropriate insulator for at least 28 days. With the failure of IDEs from 2 of the 3 SMP materials, the electrical consistency would not be provided by SMP alone, and the functional devices would require another method of creating suitable insulation.

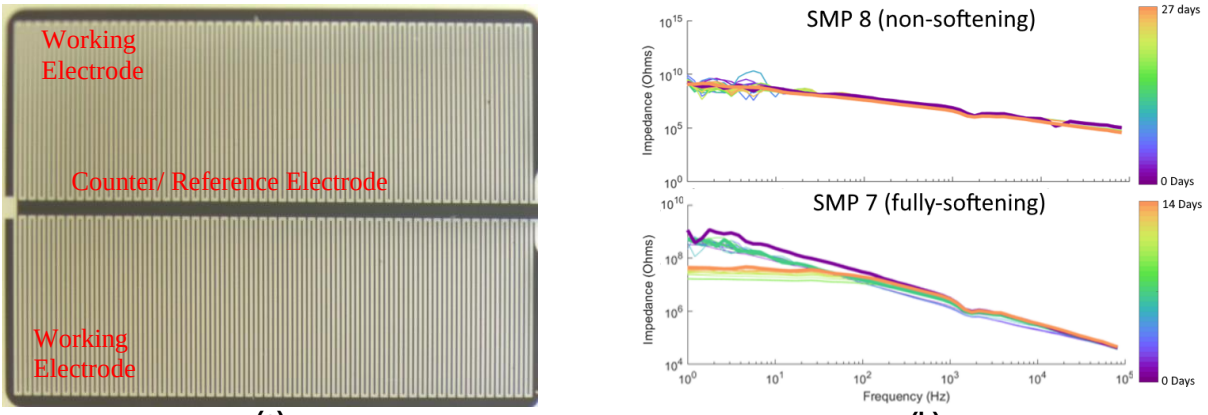

(a) (b)

Figure 6: **(a)** An optical micrograph of a SMP interdigitated electrode which contains two working electrodes. The counter and reference electrodes are common for both working electrodes. **(b)** shows representative EIS impedance spanning multiple days for the fully- and non-softening SMP IDE devices immersed in PBS at 37 °C. The SMP 7 (fully-softening) IDEs (n = 6) lasted a maximum of 7 days before the impedance fell below 1 GΩ, whereas SMP 8 (non-softening) IDEs (n = 4) maintained high impedance characteristics up until the end of the testing period at 27 days.

Our strategy is to use a multi-layer deposition process achieving an insulated pseudo-microwire within the SMP probe architecture. To this end, we have tested two materials for the interior insulation: atomic layer deposited alumina (Al_20_3) and parylene C. After fabricating IDEs with alumina over gold traces, we observed significant structural and electrical failure upon IDE immersion in PBS. ALD deposited alumina has an inherent tensile stress[3] when deposited at temperatures lower than 300 °C, and this effect is apparent in **Figure 7(a)** and **(b)**. However, temperatures above 250 °C can damage the SMP polymers, so ALD alumina was deposited at this lower temperature. Although we did not measure the actual stress within our films, the physical deformation was obvious. Our brief explanation to the failure is that the devices, once immersed in 37 °C, softened and inherent tensile stress in the ALD film proved to be a greater force that that exerted by the SMP film, thereby twisting the SMP into a tightly coiled tube for SMP 7 and a loose coil for SMP8 (**Figure 7(a)** and **(b))**. The extreme twisting of the device would lead to cracking and delamination of the ALD film from both the gold microelectrodes and the SMP, opening electrical pathways and leading to IDE failure.

[3] Miller et al. (2010) Thermo-mechanical properties of alumina films created using the atomic layer deposition technique. Sens. Actuat. A 164: 58-67.

With the failure of the ALD alumina, we looked to parylene C to provide the interior insulation. The parylene C, deposited by PECVD, does not display as much inherent tensile stress, especially compared to the alumina. The parylene C does provide a slight curvature to the device, with the bowing indicating some tensile stress, but it does not become more pronounced after immersion in PBS at 37 °C as shown in the device displayed in **Figure 7(c)**. Additionally, the parylene C also seems to provide the electrical isolation which is required of the device. **Figure 7(d)** shows impedance graphed across 20 days for an SMP 7 device with coaxial parylene C. The results from the study (n = 2) indicate that the IDE device maintained all factors above failure level. This effect was also seen with the SMP 8 formulation. Currently, a large scale SMP IDE test (n = 20) is being performed to statistically confirm that parylene C/ SMP bilayers provide, but also a reliable, homogenous electrochemical impedance.

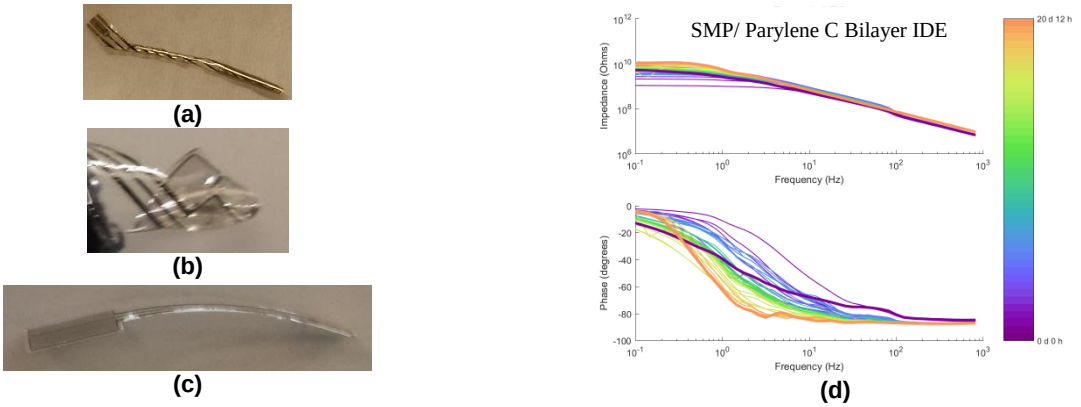

Figure 7: **(a)** Digital photograph of a SMP 7 IDE with 20 nm atomic layer deposited (ALD) alumina (AL_2O_3) interior insulation, **(b)** Digital photograph of a SMP 8 IDE with 20 nm atomic layer deposited (ALD) alumina coaxial insulation, and **(c)** a digital photograph of a SMP 7 IDE with 500 nm parylene C interior insulation. All three devices were placed in PBS at 37 °C for multiple days. The ALD IDEs failed nearly instantly when immersed in PBS, whereas the parylene C IDEs remained electrically stable and did not appreciably curled for at least 20 days in vitro. These tests are continuing.

In conclusion, we have accomplished approximately 70% of Specific Aim 2, Subtask 1. While the data are entirely promising, we are currently testing IDE structures to verify our findings that the parylene C/SMP approach will provide us with a suitable architecture going forward to complete the fabrication of SMP intracortical probes. We anticipate to have the first devices ready for implantation by November, and should have all three formulations ready and fabricated by the beginning of January 2017.

Specific Aim 2, Subtasks 2 and 3 Progress: Subtasks 2 and 3 are largely dependent on the completion of the above subtask 1. Subtask 2 involves the implantation of the microelectrode devices fabricated in subtask 1 into the motor cortex of Long-Evans rats, while subtask 3 utilizes the intracortical probes to record single units within the motor cortex of a freely moving animal as well as evaluating the implant through EIS. For these subtasks, the milestones of obtaining the IACUC and ACURO permissions has already been reached and are 100% complete. Our in vitro data suggested that metallic traces and microelectrode sites in SMP material only would not be stable in vivo. To test that idea and build laboratory experience in handling SMP based probes, we made intracortical probes with SMP 6 (non-softening) and Pt microelectrode sites and performed pilot implantations and recordings. **Figure 8(a)** shows a successful implantation of the SMP microelectrode. The procedure in short involves exposing the skull and then drilling holes and putting screws into the skull which serve as the counter/ reference electrodes and mechanical anchors for a protective head-cap (**Figure 8(b)**). A craniotomy, or removal of the skull, is performed above the motor

cortex, the dura is cut away and the SMP device is lowered into the brain (**Figure 8(c)**). With this demonstration, we are fully confident that our procedure will be sufficient to implant the electrically functional SMP probes when they are produced within the next months.

While we are behind on the surgical implantation and recording from functional intracortical probes, with the experience we have built in the laboratory, we can readily increase the number of surgeries to 3 – 4 surgeries a week, enabling us to reach the first 32 animal testing cohort within 2 months. Following this schedule, we can perform the next set of surgeries around June-July of next year and have more than 6 months for the second cohort for implantation time.

(a)

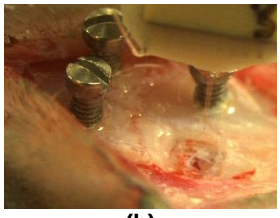

(b)

(c)

Figure 8: **(a)** Digital photographs showing a prototype SMP cortical microelectrode implanted within the motor cortex of a Long-Evans rat. The wire connected to the gold coated pin attached to the rear screw provides an additional electrical contact for the counter/ reference electrode. **(b)** A digital photograph showing the skull screws and the location of the craniotomy forward of the bregma, or the crossing points of the sagittal and coronal sutures. **(c)** A digital photograph showing the SMP probe penetrating the motor cortex of the brain.

Subtask 3 involves the recording of single units and EIS from the implanted rats two times a week. **Figure 9(a)** displays the EIS curves for 16 microelectrodes from a SMP/ Pt NNx style probe taken before implantation (Day 0) and at 4 days post implantation. The most noticeable issue with the probe, and one of the reasons the SMP implants were not ideal for single unit recordings, is there is an extreme drop in impedance, especially around the 1 KHz frequency which is the main frequency relevant for single units. This drop was due to issues discussed earlier in this section. **Figure 9(b)** displays single units obtained from a commercial NeuroNexus (NNx) A1x16 probe, and also displays the major limitation of stiff cortical implants that comprise the current state-of-the-art.

Our target time for implantation is 120 days, and at 116 days, the peak-to-peak voltage of the single unit has fallen to 30% of baseline, and by 188 days to only 6%. The issue with the NNx implant reliability is further shown in **Figure 9(c)**. This figure shows periods of bursting against the duration of the burst. 7 days after the implantation, the neuron was bursting very regularly, but the ability to either record the bursting, or the activity of the neuron itself, is greatly reduced at day 116.

Although we currently do not have any recordings of our SMP implant devices, we have shown that we can record both single units and the impedance of implanted intracortical probes. This subtask progress is currently at 0%, but will follow the implantation and recording schedule with the onset of the new implant devices.

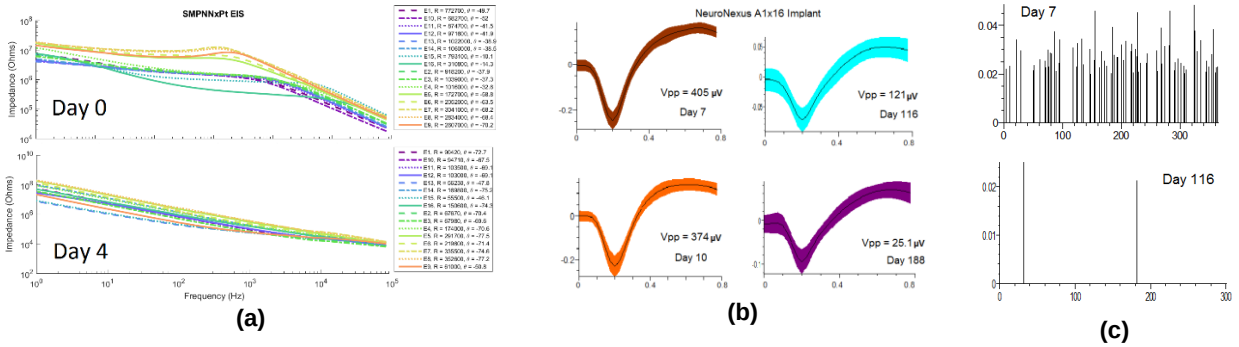

Figure 9: (a) Comparison of EIS from graph of the 16 microelectrodes from a SMP/ Pt NNx architecture probe implanted into the cortex of a Long-Evans rat. Day 0 details the impedance profiles of the microelectrode sites before implantation, while the lower set of curves is from an in vivo EIS recording. **(b)** Single unit recordings from a NeuroNexus A1x16 probe. Although there is no noticeable difference in the peak-to-peak voltage within the same week of recording, the V_{pp} falls to 30% of the original after 116 days, and 6% after 188 days. **(c)** Bursting activity of a neuron are displayed at day 7 and days 116, demonstrating the dramatic drop in recorded activity after the long term implantation period.

IMPACT

Brain electrodes are typically fabricated from conductive and insulating materials such as metals and plastics that are inherently stiff, much stiffer than the surrounding brain tissue. The neuroscience community has known that the ability of these devices to record electrical activity is lost after 6 months to 1 year after implantation. The mismatch between the stiff devices and soft brain tissue is believed to be responsible for inflammatory tissue response that plays a major role as a mechanism of failure. Our work tests the idea that if we can make a probe that softens in the brain, then the performance of the device would improve. We are capitalizing on a novel material strategy: shape memory polymers. To date, we have refined the fabrication process and have a path towards create softening devices made from SMP that leverage standard manufacturing processes that ensure reproducible. Our first publication definitively shows that the mechanical properties (i.e., degree of stiffness) of devices fabricated from a variety of SMPs tolerate ethylene oxide sterilization. The implications of this work are important in that prior studies with implantable brain electrodes have shown that incomplete sterilization causes confounds in tissue response studies and ethylene oxide is the best option. Given the broad interest in SMPs for implantable biomedical devices beyond brain electrodes, our findings have implications for more widespread biomedical use of these novel materials.

Going forward, we anticipate that we will be able to test our study's central hypothesis that softening probes induce less inflammation through tissue response and exhibit more robust neural recording. Since we are using fabrication methods that are entirely scalable for manufacturing, our efforts lay the groundwork for eventual translation towards a clinically viable device. The impact of our work on clinically deployable devices has implications for individuals living with severe neurological deficits where neurotechnology offers a path for restoration. In addition, there is widespread need in the neuroscience community interested in basic science questions for devices capable of long-term chronic recording. Implantable probes are an essential tool for the elucidation of the functional circuitry of the brain allowing simultaneously recording from neurons to elucidate modular and hierarchical processing, as well as neural circuitry involved in adaptation and learning. So, when successful, our team will provide an entirely new classes of brain electrodes that have the potential to impact the

neuroscience community to enable the pursuit of scientific questions related to brain circuitry, behavior, and learning.

CHANGES/ PROBLEMS

As highlighted in the progress report, in spite of the initial issues, we have made tremendous strides in the fabrication of functional intracortical probes comprised of SMP. We believe that we are in a great position now to ensure that data that will emerge from the study will be solid and well-founded. The delays in Specific Aim 2 subtasks are relatively minor and we will be back on schedule within the next few months.

The PI Dr. Pancrazio moved from George Mason University to the UT Dallas where Dr. Voit's group is located. This move ultimately brings the research groups together and will ensure the success of the project long term, however there was a time penalty in the short term. Transitions require re-establishing the research team and infrastructure. Moreover, Dr. Pancrazio's laboratory in the new Bioengineering and Science Building was not ready until February 2016, creating a five month delay. Progress since that time has been very brisk and so success is highly likely.

PRODUCTS

Publications:

- M. Ecker, V. Danda, A. J. Shoffstall, S. F. Mahmood, A. Joshi-Imre, C. L. Frewin, T. H. Ware, J. R. Capadona, J. J. Pancrazio, W. E., Voit, Sterilization of Thiol-ene/Acrylate Based Shape Memory Polymers for Biomedical Applications. *Macromol. Mater. Eng.* **2016**, DOI: 10.1002/mame.201600331.

Conferences:

- 2016/06/28: M. Ecker, V. Danda, J. Pancrazio, W. Voit Sterilization of softening Shape Memory Polymers used as Substrate for Neural Devices, *NANS 2 NIC - Neural Interfaces joint meeting*, Baltimore, MD (poster)
- 2016/06/28: C. Frewin, R. Modi, V. Danda, M. Ecker, R. Ayub, W. Voit, and J. Pancrazio Electrochemical Evaluation of Shape Memory Polymer Electrodes, *NANS 2 NIC - Neural Interfaces joint meeting*, Baltimore, MD (poster)
- 2016/06/28: R.Modi, W. Voit, Recent Advances in Photolithographically Defined Neural Interfaces on Softening Substrates. *NANS2-Neural Interfaces joint meeting*, Baltimore, MD, (poster)
- 2016/08/12: M. Ecker, V. Danda, J. Pancrazio, W. Voit, Thermomechanical behavior of softening shape memory polymer substrates for flexible bioelectronics before and after sterilization, *Texas Soft Matter Meeting 2016*, Richardson, TX (talk)
- 2016/08/25: M. Ecker, V. Danda, A. Joshi-Imre, J. Pancrazio, W. Voit, Understanding the material properties of implantable shape memory polymers with tunable degree of softening, *252nd American Chemical Society National Meeting & Exposition*, Philadelphia, PA (talk)

- 2016/10/07: M. Ecker, V. Danda, J. J Pancrazio, W. E. Voit, Thermomechanical Analysis of thin Shape Memory Polymer Films for Bioelectronic Medicines, *BMES - Biomedical Engineering Society - 2016 Annual Meeting*, Minneapolis, MN (poster)
- 2016/10/07: V. Danda, M. Ecker, C. L. Frewin, A. Shoffstall, J. Capadona, J. Pancrazio, W. Voit, The Impact of Sterilization on the Mechanical Properties of Thiol-ene based Shape Memory Polymers for Bioelectronic Medicines. *BMES - Biomedical Engineering Society - 2016 Annual Meeting*, Minneapolis, MN, (poster)
- 2016/10/07: R. Modi, W. Voit, Neural Interfaces with Photolithographically-defined Softening Substrates. In *BMES - Biomedical Engineering Society - 2016 Annual Meeting*, (poster)
- 2016/10/7: A. Joshi-Imre, M. Ecker, R. Modi, A. Garcia-Sandoval, W. E. Voit, Softening polymers-based bioelectronic implants. *Texas Fresh AIR,* Austin, TX, (poster)

PARTICIPANTS & OTHER COLLABORATING ORGINIZATIONS

Name: Joseph J. Pancrazio, PhD
Project Role: Principal investigator
Researcher Identifier: 0000-0001-8276-3690
Nearest Person Month Worked: 12
Contribution to Project: project administration, technical supervision of electrochemical testing of intracortical probes and in vivo recordings, supervision of post-doctoral research associate and graduate student, and coordination with the Cleveland VA Site 2.
Funding Support: University faculty and administration. With regard to new funding, since the time of this award, Dr. Pancrazio has received new support as a co-investigator for an award from DARPA BTO entitled “Advanced Materials and Fabrication Methods for Achieving Chronically Stable Recording and Stimulation with Blackrock Arrays” – there is no overlap with this CDMRP project.

Name: Walter Voit, PhD
Project Role: Co-investigator
Researcher Identifier: 0000-0003-0135-0531
Nearest Person Month Worked: 12
Contribution to Project: Overseeing shape memory polymer device fabrication, supervision of technical staff in the Cleanroom, and coordination with the PI and the Cleveland VA site.
Funding Support: University faculty.

Name: Melanie Ecker, PhD
Project Role: Post-Doctoral Research Associate
Researcher Identifier: 0000-0002-0603-6683
Nearest Person Month Worked: 6
Contribution to Project: Development and synthesis of new SMP formulations having various degrees of softening *in vivo*. Thermomechanical characterization of SMP formulations in dry and in soaked states order to verify the softening capabilities.

Investigation of the impact of various sterilization methods on the thermomechanical properties and softening on SMP formulations.
Funding Support: N/A

Name: Christopher L. Frewin, PhD
Project Role: Post-Doctoral Research Associate
Researcher Identifier: 0000-0002-7591-0629
Nearest Person Month Worked: 11
Contribution to Project: Responsible for survival surgeries, in vivo recordings, electrochemical analysis, Histological analysis, and device design.
Funding Support: N/A

Name: Alexandra Joshi-Imre, PhD
Project Role: Research Assistant Professor
Researcher Identifier: 0000-0002-4271-1623
Nearest Person Month Worked: 1.7
Contribution to Project: Research management; Microfabrication process development; Microscopy; Materials characterization; Yield analysis and Failure analysis.
Funding Support: State funded position at the UT Dallas Center for Engineering Innovation.

Name: Romil Modi
Project Role: Research Engineer
Researcher Identifier: 0000-0002-0436-7403
Nearest Person Month Worked: 5
Contribution to Project: Design and fabrication the SMP implantation devices for the project. Development of the processes required to manufacture a complete device.
Funding Support: GSK grant sub-award to Dr. Voit / Qionics

Name: Vindhya Reddy Danda
Project Role: Research Engineer
Researcher Identifier: 0000-0001-8670-8816
Nearest Person Month Worked: 10
Contribution to Project: Ms. Danda is in charge of fabricating the SMP implantation devices. She also has characterized the devices with DMA and light microscopy.
Funding Support: N/A

Name: Ms. Lisa Spurgin
Project Role: Technician
Researcher Identifier: 0000-0001-5240-2085
Nearest Person Month Worked: 2
Contribution to Project: Fabrication of shape memory polymer substrates
Funding Support: N/A

Name: Allison Stiller
Project Role: Graduate student
Researcher Identifier: 0000-0001-6326-890X
Nearest Person Month Worked: 2
Contribution to Project: Ms. Stiller performs surgeries, assists in the recording of neural signals, and analyzes the neural tissue using immunohistochemistry.

Funding Support: N/A

SPECIAL REPORTING REQUIREMENTS

As required for Collaborative awards, both PIs have submitted a report with tasks for each clearly delineated.

APPENDICES

THE UNIVERSITY OF TEXAS AT DALLAS

Office of Research Compliance

800 W Campbell Road AD15 Richardson Texas 75080-3021
972-883-4579 Fax 972-883-2310

Date: 17 December 2015

To: Joseph Pancrazio, Ph.D.
Department of Bioengineering

From: Sanaz Okhovat
Assistant Vice President, Office of Research Compliance

Re: Approval of IACUC File Number: IACUC 15-19
Title: *Comparative Performance of Novel Softening Intracortical Probes*

The IACUC protocol #15-19 has been reviewed and approved for **three** years. Please note that although the Office for Laboratory Animal Welfare (OLAW) provides for three year approvals, The United States Department of Agriculture (USDA) requires **annual** review for continuing your project.

The approval is granted from **17 December 2015** until **16 December 2018**, providing you do not change the protocol. Any changes to the protocol require submission and approval from the Institutional Animal Care and Use Committee (IACUC). The Office of Research Compliance will remind you approximately 6-8 weeks before your annual report is due. Please note, this is a courtesy reminder, and you are still responsible for submitting the annual report in a timely manner. This information must be submitted promptly after receiving this reminder in order for the IACUC to review and approve all materials requested PRIOR to the annual anniversary date of **December 16, 2016**. If your project is not received and approved before the expiration date "annually," then your project will be considered noncompliant and will need to be resubmitted as a new project. The USDA regulations require you to submit annual reports to the IACUC and final summary reports.

It is critical to point out the importance of storing, securing, and monitoring all controlled substances used for this protocol. Please refer to **UTD Policy Memorandum 97-III.27-77** or contact Laboratory Safety Manager, Kathy White at 972.883.6111, if you have any questions regarding this matter.

If you have any further questions, please contact me at 972.883.4579.

DEPARTMENT OF THE ARMY

HEADQUARTERS, US ARMY MEDICAL RESEARCH AND MATERIEL COMMAND
810 SCHREIDER STREET
FORT DETRICK, MD 21702-5000
February 02, 2016

REPLY TO ATTENTION OF

Director, Office of Research Protections
Animal Care and Use Review Office

Subject: Review of USAMRMC Proposal Number PR141308, Award Number W81XWH-15-1-0607 entitled, "The Effect of the Elimination of Micromotion and Tissue Strain on Intracortical Device Performance"

Principal Investigator Joseph Pancrazio
University of Texas, Dallas
Richardson, TX

Dear Dr. Pancrazio:

Reference: (a) DOD Instruction 3216.01, "Use of Animals in DOD Programs"
(b) US Army Regulation 40-33, "The Care and Use of Laboratory Animals in DOD Programs"
(c) Animal Welfare Regulations (CFR Title 9, Chapter 1, Subchapter A, Parts 1-3)

In accordance with the above references, protocol PR141308 entitled, "Comparative Performance of Novel Softening Intracortical Probes," IACUC protocol number 15-19, Protocol Principal Investigator Joseph Pancrazio, is approved by the USAMRMC Animal Care and Use Review Office (ACURO) as of 01-FEB-2016 for the use of rats and will remain so until its modification, expiration or cancellation. This protocol was approved by the University of Texas, Dallas IACUC on 17-DEC-2015.

Required Actions: When updates or changes occur, documentation of the following action or events must be forwarded immediately to ACURO:

- IACUC-approved modifications, suspensions, and triennial reviews of the protocol (All amendments or modifications to previously authorized animal studies must be reviewed and approved by the ACURO prior to initiation.)

- IACUC actions involving this protocol regarding
  a. any noncompliance;
  b. any deviation from the provisions of the Guide for the Care and Use of Laboratory Animals; or
  c. any suspension of this activity by the IACUC

- USDA or OLAW regulatory noncompliance evaluations of the animal facility or program

Sterilization of Thiol-ene/Acrylate Based Shape Memory Polymers for Biomedical Applications

Melanie Ecker,* Vindhya Danda, Andrew J. Shoffstall, Samsuddin F. Mahmood, Alexandra Joshi-Imre, Christopher L. Frewin, Taylor H. Ware, Jeffrey R. Capadona, Joseph J. Pancrazio, Walter E. Voit*

A fundamental study on the sterilization of thiol-ene/acrylate polymers for biomedical applications is presented. These polymer networks belong to the emerging field of shape memory polymers and have the capability to undergo softening after insertion into the body. The impact of various sterilization methods, such as radiation, steam, and ethylene oxide on the thermomechanical properties of these stimuli responsive materials is investigated. Time and temperature dependent thermomechanical properties of sterilized and nonsterilized samples are determined by means of dynamic mechanical analysis in an aqueous environment to allow testing of polymers in phosphate buffered saline. The findings show that ethylene oxide sterilization is appropriate for thiol-ene and thiol-ene/acrylate based shape memory polymers. This method does not adversely affect thermomechanical and self-softening properties and after sterilization, endotoxin levels remain below the thresholds recommended in the FDA Guidance.

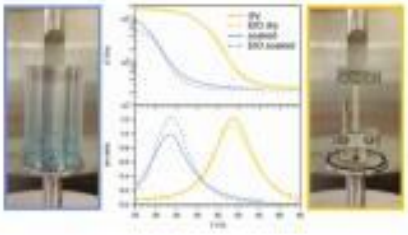

Dr. M. Ecker, V. Danda, Dr. A. Joshi-Imre, Prof. W. E. Voit
Department of Materials Science and Engineering
The University of Texas at Dallas
800 W. Campbell Rd., Richardson, TX 75080, USA
E-mail: melanie.ecker@utdallas.edu; walter.voit@utdallas.edu
V. Danda, Dr. C. L. Frewin, Prof. T. H. Ware, Prof. J. J. Pancrazio, Prof. W. E. Voit
Department of Bioengineering
The University of Texas at Dallas
800 W. Campbell Rd., Richardson, TX 75080, USA
Dr. A. J. Shoffstall, Prof. J. R. Capadona
Department of Biomedical Engineering
Case Western Reserve University
2071 Martin Luther King Jr. Drive, Cleveland, OH 44106, USA
Dr. A. J. Shoffstall, Prof. J. R. Capadona
Advanced Platform Technology Center
Louis Stokes Cleveland Department of Veterans Affairs Medical Center, 10701 East Blvd, 151 W/APT, Cleveland OH 44106-1702, USA
Dr. S. F. Mahmood, Prof. W. E. Voit
Department of Chemistry and Biochemistry
The University of Texas at Dallas
800 W. Campbell Rd., Richardson, TX 75080, USA

1. Introduction

Polymers and polymer-composites are increasingly used for in vivo biomedical applications and have become an indispensable part of modern medicine.[1] This is attributed to their versatility: polymers can be designed and prepared with a wide variety of structures with customized physical, chemical, and surface properties. Applications include, but are not limited to, polymeric therapeutics and diagnostics, dental implants, catheters, joint replacements, ligaments, vascular grafts, and heart valves.[2]

Polymer classes used for biomedical applications include biodegradable polymers,[3] polymeric micelles and vesicles,[4] nanoparticles,[5] hydrogels,[6] and dendrimers.[7] Recently, shape memory polymers (SMPs) have been under extensive investigation for their use for biomedical applications.[8]

In general, SMPs are stimuli responsive materials.[9] They have the capability to change their shape in response to certain external stimuli, such as temperature, electricity, magnetic fields, pH, or moisture. Beyond that,

their phase (and thus, their shape) transition temperature can be shifted in response to plasticizing effects of solvents, including water, resulting in a lower modulus at a given temperature. With regard to biomedical applications, current studies focus on surgical and implantable devices for therapeutics and diagnosis, such as self-expanding stents,[10] intelligent sutures,[11] active catheters,[12] and microscale neural interfaces.[13] In fact, our group focuses on the development and demonstration of self-softening devices for recording and stimulation of neural systems, taking advantage of the thermomechanical properties of SMPs.[14] The principle of these devices is that they are rigid (glassy) during insertion but become elastic (rubbery) during use to minimize the modulus differential between neural tissue and the device that has been associated with neuroinflammation.[15]

Medical devices undergo sterilization to be used in clinical environments in order to remove various microorganisms.[16] Established methods, which are listed in the FDA Guidance[17] include steam, ethylene oxide (EtO), and radiation.[16,18] However, these techniques may influence the material properties of the polymers significantly. Therefore, it is important to study the physical impact of the sterilization methods on medical devices,[19] especially on heat sensitive materials such as SMPs, which may alter their thermomechanical properties.[20] Hence, it is no surprise that in 2014, Wong et al. raised significant concerns about the biomedical practicality of SMPs, given the uncertainties related to sterilization.[21]

In this paper, we examine the effects of sterilization on the thermomechanical properties of neural probe test structures comprised of SMP. We verify sterilization efficacy by performing chromogenic residual endotoxin assays with samples composed of SMP formulations. Our findings indicate that SMPs composed of thiol-ene and thiol-ene/acrylates are sensitive to various sterilization approaches, where shifts in transition temperature and modulus are evident. We show that with the use of a mild plasma etch prior to steam and EtO sterilization, the SMP based test devices exhibit homogenous mechanical behavior that is consistent with well-defined polymer network structures. The overall procedure does not affect the functionality of the SMPs, such that the test devices still undergo controlled softening after immersion in aqueous solution.

2. Results

2.1. Fabrication of SMP Test Devices

To create SMPs which could undergo different degrees of softening, we prepared thiol-ene (SMP-FS, fully softening) and thiol-ene/acrylate (SMP-SS, slightly softening) polymers with stoichiometric thiol to ene contents using photoinitiated thiol-ene click chemistry (Scheme 1).[22] In order to mimic the conditions actual devices would undergo, both SMP substrates were photolithographically defined using cleanroom processing methods such as nitride deposition, plasma, and hydrofluoric acid (HF) etch to receive rectangular specimens having dimensions of 4.5 mm × 50 mm × 30 µm. Some of the samples were subjected to an additional oxygen plasma etching step before they were singulated. This removed ≈4 µm of the top surface but was accompanied by the nontransparent, milky appearance of the samples due to light scattering at the roughened surface.

In contrast to prior studies, where cast samples with thicknesses in the mm range were used for thermomechanical investigations due to a limitation of traditional techniques in their ability to measure thin films,[14a,c] we herein prepared spin coated samples in the µm thickness range, which is the thickness of devices used for in vivo studies. Unexpectedly, the thermal and mechanical

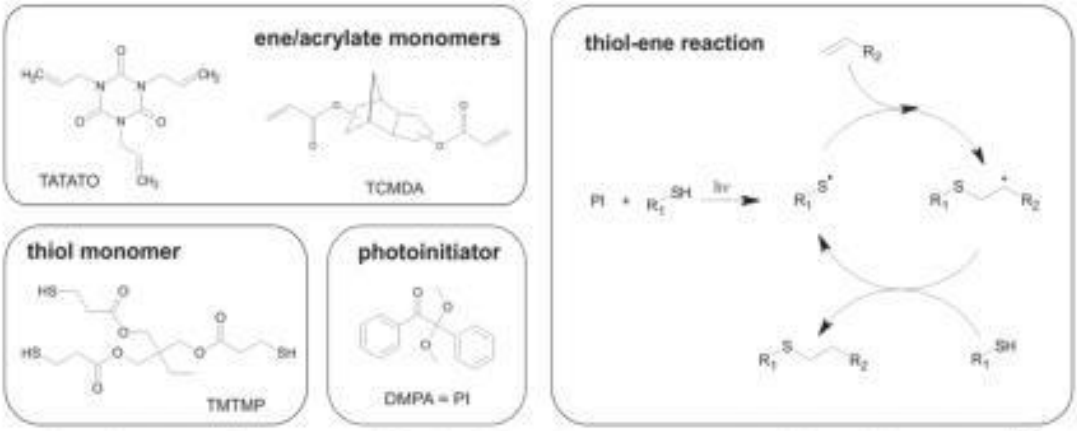

Scheme 1. Chemical structures of monomers used for the different polymer compositions and the used photoinitiator (left) and scheme of thiol-ene reaction (right).

properties were strongly dependent on the preparation method. The T_g of cast samples was significantly lower than spin coated samples having the same monomer composition. This might be explained by different curing scenarios: namely, the cast samples were covered by a glass slide which absorbs a part of the UV radiation and thus leads to lower energy transfer to the polymer solution including the photoinitiator compared to the spin cast samples which were uncovered. In addition, the exposure of the polymer solution to oxygen as part of the atmosphere in case of the spin cast samples might influence the cross-linking behavior as well. It is known, that oxygen can inhibit the cross-link reaction of acrylates.[23] In case of the thiol-ene reaction, oxygen is not acting as inhibitor, but however can be incorporated into side chains of the polymer network through a well-described mechanism.[24] In order to eliminate possible effects caused by oxygen, some samples were cured under varied curing scenarios, namely irradiation under 254 nm for 2 h under nitrogen and argon atmosphere instead of air. The thermomechanical properties of SMP-FS after the different curing scenarios are shown in Figure 1. The properties did not significantly differ from each other after curing under varied atmospheres, indicating that the presence of oxygen during the curing did not influence the bulk thermomechanical properties of thick polymer networks. However, a removal of the top 4 µm from the top surface by an oxygen plasma etch changed the polymer properties noticeably. The drop in modulus was more pronounced and the glass transition region was narrower, which is representative of more homogenous networks as prior to etching. This surface treatment was used prior to all following sterilization procedures in order to assure consistent conditions.

In addition, the differences in surface chemistries before and after etching were investigated by means of attenuated total reflectance Fourier transform infrared spectroscopy (ATR-FTIR) (shown in Figure S1, Supporting Information). The oxygen plasma etching resulted in an increased absorbance from 3580 to 3060 cm^{-1}, which is attributed to hydroxyl groups. Beyond that, the peaks at 2961, 2926, and 2854 cm^{-1}, which are attributed to asymmetrical and symmetrical CH stretching vibration of CH_3 and CH_2 groups, increased noticeably. The rest of the spectra showed no significant changes. This observation indicates that the oxygen plasma etching causes changes in the number of the alkyl and hydroxyl groups within the polymer surface, possibly through bond breaking, formation of radicals, and reformation of new bonds.[25]

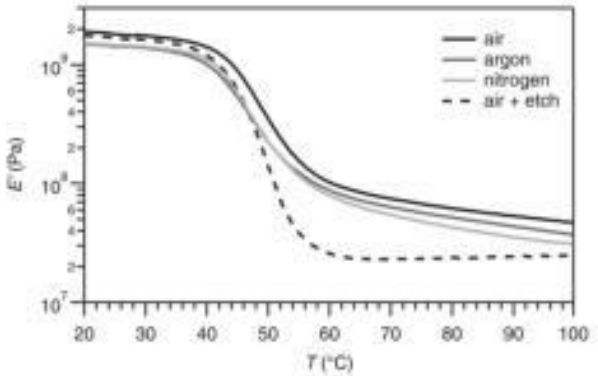

Figure 1. DMA measurements of SMP-FS samples after curing in different atmospheres, namely air, argon, and nitrogen. The dashed graph shows the storage modulus E' of a sample cured under air, but with postetching of the first 4 µm.

2.2. Sterilization of SMP Test Devices

Surface etched SMP samples were subjected to different sterilization methods. All specimens were mounted in a manner that they were hanging downward and were free floating (not attaching any surface) in order to prevent them from bending or twisting. The impact of sterilization on thermomechanical properties appeared to depend on the sterilization method rather than on the polymer composition. For example, SMP-FS and SMP-SS showed similar shifts in T_g after EtO exposure (Figure 2). In addition, the surface properties of the SMP samples were investigated by means of ATR-FTIR spectroscopy to see if there are any changes caused by the sterilization procedures (Figure 3). The IR spectra of both investigated SMP networks showed only minor changes in the peak intensities after the applied sterilization methods. This suggests that sterilization does not alter the chemical properties of the SMP materials.

2.2.1. UV Sterilization

After 120 min of UV irradiation at 254 nm, the glass transition region was less narrow than for neat samples (Figure 2). At the same time, the characteristics of the drop in storage modulus E' when passing the glass transition region changes drastically where the curve shows a two-fold transition. The initial modulus change was similar to neat samples, but after 8–10 °C the slope changed to a smaller value. In the tan δ curves of the UV sterilized samples, there was also a second, less distinct but broad peak/plateau visible. In case of the SMP-FS, the second T_g was found around 68 °C, in case of the SMP-SS the tan δ curve remained at a plateau after the T_g peak. However, the main T_g remained almost unaffected at the same temperature.

These findings indicate that the resulting polymer network within the sample is inhomogeneous. In order to verify whether this behavior was due to any plasticizing effects caused by the ethanol dip prior to UV exposure, we also investigated the material properties for UV treatment only. The effects appeared to not be related to the ethanol dip, since the modulus followed the same characteristics

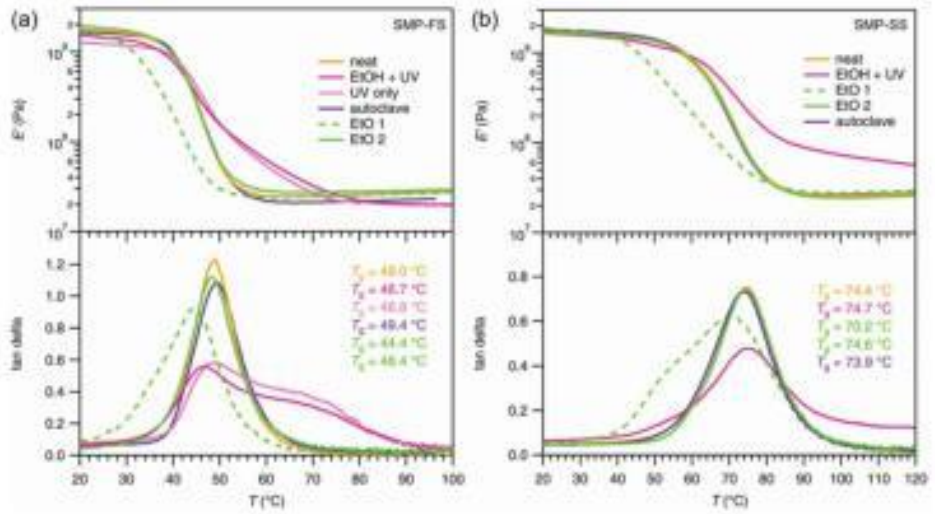

Figure 2. DMA measurements of the a) SMP-FS and b) SMP-SS samples after surface etch followed by various sterilization methods. Top shows the storage modulus E', the bottom the tan δ, respectively.

in both cases. However, a removal of the top 4 µm from the UV exposed surface by an additional oxygen plasma etch changed the overall materials properties back to a uniform glass transition (not shown herein). This observation suggests that the bulk properties remained unaffected while the surface properties were changed by the intense UV irradiation.

2.2.2. Autoclave

The thermomechanical properties of the different polymer compositions were not affected by the autoclave sterilization, which includes exposure to steam at 121 °C followed by a drying cycle. The temperature dependent storage modulus E' did not show any significant differences after treatment with steam and pressure as visible by almost congruent dynamic mechanic analysis (DMA) curves (Figure 2). Beyond that, no shift in T_g was evident, indicating that the SMPs are stable with respect to their network structures and hence with their thermomechanical properties as well.

2.2.3. Ethylene Oxide

When measuring DMA of SMP samples shortly after sterilization with EtO gas, the glass transition region broadened and T_g shifted 5–7 °C toward lower temperatures (dashed green lines in Figure 2). The storage modulus E' of both SMPs remained the same in the glassy state (at temperatures below the T_g) as well as in the rubbery regime (at temperatures above T_g) post sterilization. However, when repeating the same DMA measurements on samples sterilized at least 7 d prior to measurement on the DMA, the T_g shifted back to the value of nonsterilized samples (solid green lines in Figure 2). This observation suggests that EtO gas has a reversible plasticizing effect on the polymer, and that the exposed SMP samples need a longer aeration phase for removal of EtO gas as compared to other materials. The degassing time could be reduced to 3 d by keeping the samples under low vacuum (0.62 bar). It might be possible that the degassing time could be reduced even further by simultaneously increasing the temperature.

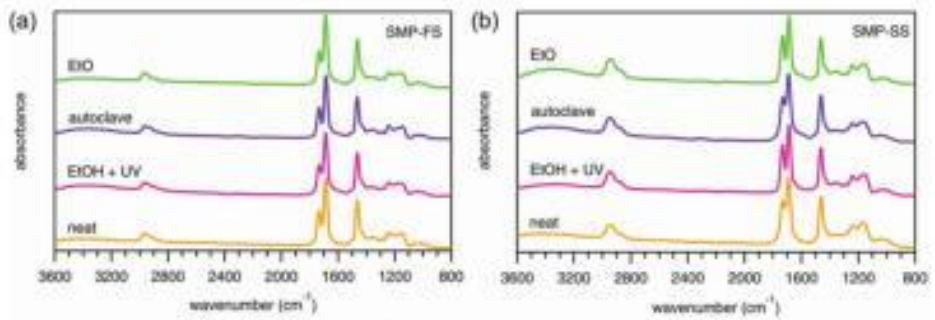

Figure 3. Normalized ATR-FTIR spectra of surface etched a) SMP-FS and b) SMP-SS samples after various sterilization methods.

Macromolecular Journals
Macromol. Mater. Eng. **2016**, DOI: 10.1002/mame.201600331

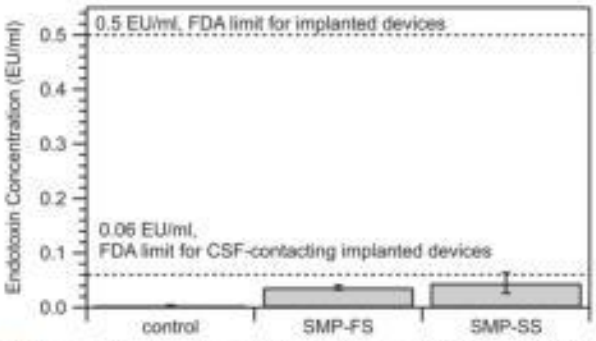

Figure 4. Results of endotoxin testing for SMP-FS and SMP-SS samples after sterilization with EtO. Control sample is certified endotoxin-free water exposed to the incubation period, handling, and preparation as the test devices. Thresholds of acceptable endotoxin concentration (EU mL^{-1}) limits, as set forth by FDA Guidance for Industry for implantable devices, are indicated by horizontally dashed lines.

In order to further investigate this phenomenon, we performed ATR-FTIR measurements on samples before and after EtO sterilization. We observed only minor changes in the surface chemistry of the SMP (Figure 3). The broad peak at 3580–3060 cm^{-1} was slightly increasing, indicating the incorporation of hydroxyl groups. Since the ATR-FTIR measures only surface effects, we also extracted the remaining EtO from sterilized SMP-FS samples in acetone after different degassing times and performed ^{1}H-NMR spectroscopy (shown in Figure S2, Supporting Information). Directly after the sterilization, a peak at 2.6 ppm was evident. This peak diminished significantly after additional degassing time.

2.3. Endotoxin Measurements of Sterilized Test Devices

Endotoxin tests were performed on SMP-FS and SMP-SS test devices that were sterilized by EtO using a 24 h cycle, followed by 15 d of outgassing under standard ambient temperature and pressure. Both samples showed minimal endotoxin contamination, achieving levels below the threshold suggested in the FDA Guidance for Industry for cerebrospinal fluid (CSF)-contacting implanted devices (0.06 EU mL^{-1}, Figure 4).[26] In particular, the samples revealed values of 0.037 (SMP-FS) and 0.045 EU mL^{-1} (SMP-SS), respectively.

2.4. Soaking of Neat and Sterilized SMP Test Devices in Phosphate Buffered Saline (PBS)

We investigated the soaking behavior of the different SMP compositions before and after sterilization. DMA measurements were performed using the RSA-G2 with Immersion System (Figure 5).

The specimens were clamped, the PBS added, and the measurement was started immediately. The first step consisted of rapid heating from room temperature to

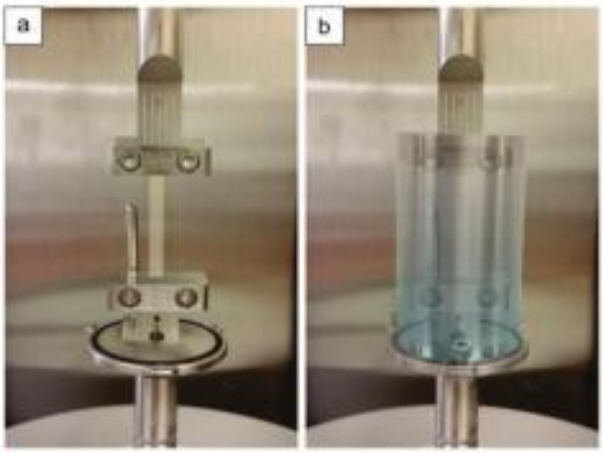

Figure 5. Setup for a) dry and b) immersed DMA measurements.

37 °C followed by isothermal soaking of the polymer films (Figure 6). The second step included cooling from 37 to 20 °C followed by application of a heating ramp from 20 to 70 °C while still immersed in PBS (Figure 7). As expected, the aqueous environment altered the mechanical properties of the SMP. For both compositions, the storage modulus E' dropped noticeably after 10–20 min immersion in PBS at 37 °C, for the fully softening SMP more pronounced than for the slightly softening SMP (Figure 6). After the initial drop, the modulus remained at a constant plateau for the remaining soaking interval. The behavior before and after sterilization with EtO was

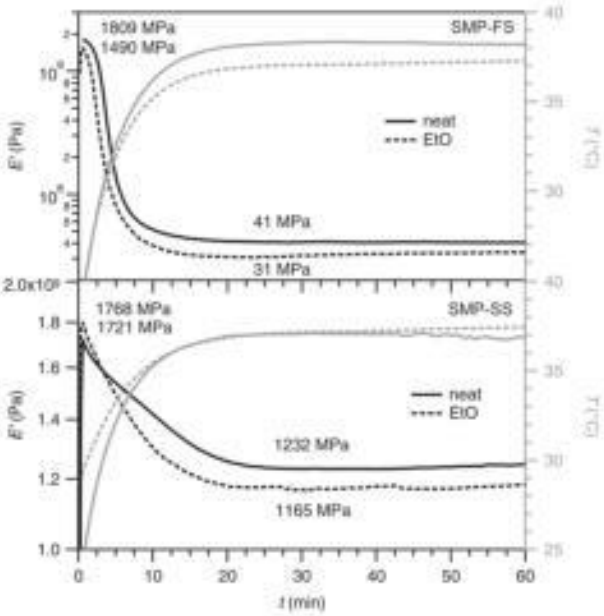

Figure 6. DMA measurements of surface-etched SMP-FS (top) and SMP-SS (bottom) before and after EtO sterilization. Shown are the storage modulus E' (black) and the respective temperature (grey) during soaking in PBS over the immersion time.

Macromol. Mater. Eng. **2016**, DOI: 10.1002/mame.201600331

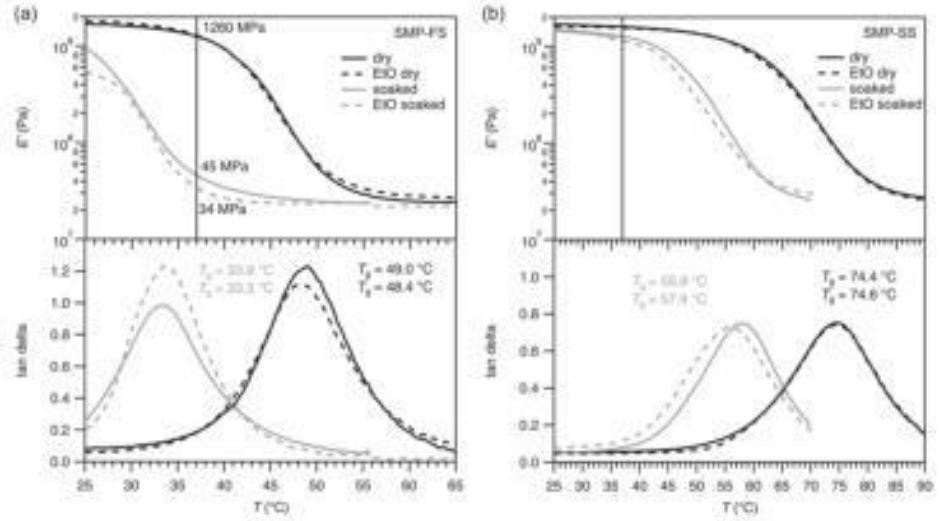

Figure 7. DMA measurements of surface-etched a) SMP-FS and b) SMP-SS before and after EtO sterilization. Showing the storage modulus E' (top) and the tan δ (bottom) of dry (black) and of in PBS soaked (grey) samples, respectively. Vertical line indicates the values at 37 °C.

similar. The modulus of nonsterilized SMP-FS dropped from 1809 MPa at room temperature directly after insertion to 41 MPa after 20 min in PBS at 37 °C, whereas the modulus of sterilized SMP-FS dropped from 1490 to 31 MPa. For the SMP-SS, E' dropped from 1768 to 1232 MPa before, and from 1721 to 1165 MPa after sterilization. After 60–120 min soaking in PBS, the T_g of both compositions was observed to decrease by 15–20 °C compared to the dry values (Figure 7). The glass transition temperature for nonsterilized SMP-FS (control) dropped from 49.0 to 33.3 °C; the sterilized SMP-FS dropped from 48.4 to 33.9 °C. The T_g values for the nonsterilized SMP-SS samples changed from 74.6 to 57.9 °C, whereas the sterilized samples changed from 74.4 to 55.9 °C. The storage moduli in the glassy and rubbery states after soaking have been almost the same for both compositions, before and after sterilization with EtO. The only difference was observed for the SMP-FS at 25 °C, where the glassy modulus for sterilized samples was lower (540 MPa) as for the nonsterilized equivalents (950 MPa). This might be caused by plasticization effects, but has no impact to the functionality of devices since these are values of soaked samples. For dry samples, the storage modulus in the glassy state is in any case high enough for a reliable handling during insertion. Although the maximum temperature to which the immersed samples could be heated was limited to 70 °C, which was attributed to the experimental setup, this was high enough to verify the tan δ peak and the rubbery modulus of both compositions after softening because the glass transition of both polymers was within this temperature range.

The softening characteristics of the herein tested thiol-ene and thiol-ene/acrylate were not impaired. This indicates, that sterilization with EtO gas has insignificant influence on modulus as a function of temperature and does not affect the degree of softening of the SMP.

3. Discussion

We have shown for the first time that SMP-based structures designed for neural implantation tolerate sterilization procedures necessary for reliable preclinical studies and eventual clinical use.

One key challenge, when using biomedical devices in vivo, is their proper sterilization. A common way to sterilize temperature sensitive polymeric devices is the use of 254 nm UV light. However, the thermomechanical properties of SMP-SF and SMP-SS were significantly affected through the UV treatment (Figure 2). The inhomogeneity between surface and core could be explained by accelerated ageing effects of the polymer caused by irradiation for 2 h at 254 nm. These include chain scissions and formation of new bonds. In particular, thioether bonds are relatively weak and are known to be susceptible to photoinduced cleavage.[27] Further investigations would be necessary to clarify the specific underlying mechanisms in these particular networks.

In contrast, sterilization with steam and EtO did not significantly affect the thermomechanical properties of the SMP test devices or their surface characteristics as demonstrated by DMA (Figure 2) and ATR-FTIR (Figure 3) measurements, respectively. These findings are in line with the findings of Yakacki et al.,[20] who studied the thermomechanical behavior of acrylate-based SMPs after various sterilization methods.

However, with regard to the fabrication of functionalized devices, steam sterilization is inappropriate. The deposited metals and electronic connecters might be corroded by the harsh conditions. From a more general viewpoint, it would also be difficult to sterilize temporary deformed SMPs having a transition temperature below 120 °C without triggering the shape memory effect.

Unlike sterilization by steam, EtO sterilization is performed at low temperatures and therefore more suitable for temperature sensitive materials such as SMP. Even though the T_g is depressed shortly after sterilization by a few degrees due to plasticization, this effect was shown to be reversible (Figure 2). After an extended degassing step, the material behaved the same as before sterilization.

Sterilization methods, including EtO, steam, and dry heat, were previously tested to compare their ability to remove endotoxins from silicon microelectrodes. Ravikumar et al. demonstrated that decreased levels of endotoxin contamination left on sterilized implants directly corresponded to decreases in acute neuroinflammation surrounding microelectrodes implanted in mice brains.[28] Specifically, EtO gas sterilized implants had less residual endotoxins, resulting in less neurodegenerative effects than autoclaved or heat treated implants. Consequently, we strived to apply an EtO-based sterilization method for SMP devices. In fact, SMP-FS and SMP-SS met the FDA-recommended criteria for maximum residual endotoxin concentration for CSF-contacting implanted devices (<0.06 EU mL^{-1}) (Figure 4).

With regard to the application of SMP as softening neural probes, equally as relevant as the room temperature behavior of dry test devices, is their behavior under conditions representative of in vivo use. Therefore, we soaked the test devices before and after sterilization in PBS at 37 °C and monitored the change of their thermomechanical properties. The water uptake accompanied rapid reduction of both the modulus and glass transition temperature, faster than prior studies.[13b] After 10 min of immersion, the storage modulus of SMP-FS decreased by two orders of magnitude, while the modulus of SMP-SS decreased just by a few hundred MPa (Figure 6), which is in line with the proposed softening characteristics of the individual polymers. For both compositions, the modulus was stabilized at a plateau after 15–20 min, and therefore the softening of the SMP test devices was considered to be complete. This gives the surgical timeframe for the reliable insertion of devices (~10 min) into the body before they become too elastic and may buckle when attempting to penetrate tissue. The values for the EtO sterilized samples were comparable to the non-sterilized equivalents, showing that the degree of softening and the time required for plasticization, was not impaired.

The second part of the measurement of the soaked samples comprised a heating ramp from 20 to 70 °C to validate the material properties after plasticization caused by the aqueous solution (Figure 7). It is widely known that molecular interaction between water and the polymer chains leads to increased free volume which allows increased chain segment mobility.[29] As expected from prior studies with similar thiol-ene and thiol-ene/acrylate networks,[13b] the shift in T_g from the dry to the soaked state was ≈15 °C for both, the fully softening and the slightly softening SMP. Once again, the sterilization with EtO gas had only a minor influence on the thermomechanical properties of the herein tested thiol-ene and thiol-ene/acrylate, showing that the functionality of the SMP was not affected. Thus, this sterilization method seems to be promising for functionalized devices using the herein presented SMPs as a substrate. However, the properties of fully functionalized and packaged devices may differ from the herein investigated test structures, and therefore it is important to investigate in how far sterilization has an impact on the electrical behavior and overall performance on bioelectronic devices.

4. Conclusions

We have demonstrated that softening SMPs composed of either thiol-ene or thiol-ene/acrylate networks are compatible with various sterilization methods. In particular, the treatment with EtO gas did not damage thin photolithographically defined polymer films and seems to be a promising method to sterilize softening neural probes. Using DMA equipped with an immersion system, we observed that EtO sterilized samples showed only minor changes in their thermomechanical properties, and more importantly, the engineered softening behavior of SMPs was not impaired. In addition, sterilization of the samples met the FDA Guidance for residual endotoxin concentrations. Our findings have significant implications for the commercial biomedical application of SMP-based devices including neural electrodes. By building sterilization methods into our fabrication processes and factoring sterilization effects into material design, the biomedical application potential of novel materials such as SMPs can be realized.

5. Experimental Section

5.1. Polymer Solutions

1,3,5-Triallyl-1,3,5-triazine-2,4,6(1H,3H,5H)-trione (TATATO), tricyclo[5.2.1.$0^{2,6}$]decanedimethanol diacrylate (TCMDA), trimethylolpropane tris(3-mercaptopropionate) (TMTMP), 2,2-dimethoxy-2-phenylacetophenone (DMPA) were purchased from Sigma-Aldrich (Scheme 1). All the chemicals were used as received without further purification.

Two SMP compositions were prepared, a thiol-ene and a thiol-ene/acrylate, each consisting of stoichiometric quantities of thiol to ene functionalities. Exact mole fractions were: TMTMP-TATATO = 0.5-0.5 (SMP-PS) and TMTMP-TATATO/TCMDA = 0.345-0.345/0.31 (SMP-SS). A total of 0.1 wt% DMPA of total monomer weight was dissolved in the solution for the initiation of the photopolymerization of the monomer solution. The vial was covered in aluminum foil to prevent incident light from contacting the monomer solution and kept at room temperature. Without exposing the solution to light, the vial was mixed thoroughly by planetary speed mixing.

5.2. Sample Preparation

The polymer solutions were spin cast on 75 mm × 50 mm glass microscope slides using a Laurell WS-650-8B spin coater. Spin speed was 600 rpm and time was 30 s for SMP-PS and 25 s for SMP-SS in order to achieve thicknesses of about 30 µm, respectively. Polymerization was performed at ambient temperature using an UVP CL-1000 cross-linking chamber with five overhead 254 nm UV bulbs for 120 min under air. In addition, some samples were cured in the UV chamber floated with either nitrogen or argon gas. Cured samples were then placed in a vacuum oven at 120 °C and five in Hg for 24 h to further complete network conversion.

5.3. Nonfunctional Devices

Test devices were fabricated in the UT Dallas Class 10 000 cleanroom facility. The above SMP-on-glass substrates were used as the starting substrates in the cleanroom. Low temperature silicon nitride (using PlasmaTherm-790 plasma-enhanced chemical vapor deposition (PECVD)) was deposited to act as a hard mask for the following plasma etching processes in which the device outline/shape was patterned. Adjacently, the nitride hard mask was etched away in the 1:10 HF dip. For some SMP samples, top 4 µm thick crust was etched away in oxygen plasma (Technics reactive ion etch (RIE)). In a final step, the test devices having dimensions of 4.5 mm × 50 mm × 30 µm were delaminated from the glass slide by soaking in water.

5.4. DMA

DMA was performed using a TA RSA-G2 with Immersion System in tension mode in order to quantify the storage modulus E' and tan δ of dry or in PBS soaked samples (Figure 5). All measurements were performed on rectangular samples as received after the cleanroom processing, having a width of 4.5 ± 0.1 mm and thicknesses of 30 ± 3 µm. The following parameters were selected: clamping distance of 15 mm, a preload force of 0.05 N, a frequency of 1 Hz, and a deformation amplitude of 0.275% strain. Dry experiments were run from 10 to 100 °C or from 20 to 120 °C using a heating rate of 2 °C min^{-1}. Soaking experiments were run using the immersion system of the RSA-G2 filled with PBS. The first step (the soaking) included the heating from room temperature to 37 °C followed by isothermal oscillating for 60 or 120 min. The second step comprised first cooling down to the start temperature with a rate of 3 °C min^{-1} followed by heating from 10 to 80 °C applying a heating rate of 2 °C min^{-1}. It should be noted, that there was an offset of about 10 °C between the set temperature and the measured temperature inside the solution, based on the experimental setup. All measurements were performed on three independent specimens in order to gather statistical results.

5.5. Infrared Spectroscopy

ATR-FTIR measurements were performed with an IRAffinity-1 spectrometer from Shimadzu using a deuterated, L-alanine doped triglycine sulfate (DLATGS) detector. The ATR cell was equipped with a ZnSe crystal. The spectra were recorded from 4000 to 800 cm^{-1} as the average of 32 scans at a resolution of 2 cm^{-1}. Analysis of data included baseline correction, ATR correction, and normalization.

5.6. UV Sterilization

Specimens were dipped in ethanol (EtOH) and immediately transferred to a UV chamber equipped with five overhead 254 nm UV bulbs, in which they were irradiated for 120 min.

5.7. Autoclave Sterilization

Specimens were mounted inside containers and loaded into a Getinge 400/500LS-E series steam sterilizer. Small strips of autoclave indicator tape were applied to the containers before they were placed into the autoclave. Superdry cycle was selected, which includes exposure to steam for 30 min at 121 °C and 15 psi, followed by 75 min drying cycle. Post sterilization cycle, the stripe color of the indicator tape was inspected to verify whether or not the desired temperature of 121 °C was reached.

5.8. Ethylene Oxide Sterilization

Specimens were mounted inside appropriate size glass petri dishes, sealed, and loaded into a liner bag along with gas indicator tape and biological indicators, such as a Dosimeter and a Steritest. Next, the packed samples were loaded into the ethylene oxide sterilizer (AN 74i, Anprolene, Andersen Sterilizers Inc.) along with a Humidichip to ensure a minimum of 35% relative humidity inside the sterilization liner bag. After a minimum of 4 h of prehumidification, the glass ampoule containing 18 g of liquid EtO was added to the liner bag which was then sealed using velcro wrap. The room temperature and atmospheric pressure 24 h sterilization cycle was then started and samples were retrieved after the 2 h purge/aeration and degassing cycles following sterilization, to remove the residual EtO. All indicators were inspected for color changes to make sure the gas came in contact with the specimens.

5.9. Measurement of Residual Endotoxins

A Kinetic-QCL chromogenic limulus amebocyte lysate (LAL) endotoxin assay (Lonza, Inc., Catalog Number: 50-650U) was used to determine the level of residual endotoxins on the surface etched SMP test devices after EtO sterilization. The Kinetic-QCL assay was a quantitative assay for the detection of

gram-negative endotoxins. Endotoxin level was indirectly measured as a function of the reaction time associated with endotoxin-activation of an enzyme that catalyzed the release of the chromogen p-nitroaniline.

Three independently prepared test devices were assayed, in triplicate, for each SMP composition ($n = 3$). Residual endotoxins were extracted from test devices via incubation with certified endotoxin-free water for 24 h at 37 °C (LAL Reagent Water, Lonza). All glassware and handling instruments were rendered endotoxin-free by dry heat or EtO prior to use. Endotoxin activity on a given microelectrode sample was calculated from a five-point log–log standard curve generated from the Kinetic-QCL kit following methods described by the vendor (Lonza). Negative (blank) controls confirmed the absence of contamination from handling and preparation of the assay. A positive-spike control test confirmed that the SMP materials did not interfere with the assay.

Supporting Information

Supporting Information is available from the Wiley Online Library or from the author.

Acknowledgements: This work was supported by the Office of the Assistant Secretary of Defense for Health Affairs through the Peer Reviewed Medical Research Program under Award Nos. W81XWH-15-1-0607 and W81XWH-15-1-0608. Opinions, interpretations, conclusions, and recommendations were those of the authors and were not necessarily endorsed by the Department of Defense. Additionally, the contents did not represent the views of the U.S. Department of Veterans Affairs or the United States Government.

Received: July 26, 2016; Revised: September 8, 2016; Published online: ; DOI: 10.1002/mame.201600331

Keywords: biocompatibility; shape memory polymers; sterilization; stimuli-sensitive polymers; thermomechanical properties

[1] A. S. Kulshrestha, A. Mahapatro, in *Polymers for Biomedical Applications*, American Chemical Society, Washington, DC **2008**, p. 1.
[2] a) D. F. Williams, *Biomaterials* **1981**, *2*, 133; b) S. Ramakrishna, J. Mayer, E. Wintermantel, K. W. Leong, *Compos. Sci. Technol.* **2001**, *61*, 1189; c) R. Duncan, *Nat. Rev. Drug Discovery* **2003**, *2*, 347; d) L. Hartmann, S. Haefele, R. Peschka-Suess, M. Antonietti, H. G. Borner, *Chem. - Eur. J.* **2008**, *14*, 2025; e) A. Bertin, *Macromol. Chem. Phys.* **2012**, *213*, 2329.
[3] a) R. W. Lenz, *Adv. Polym. Sci.* **1993**, *107*, 1; b) L. S. Nair, C. T. Laurencin, *Prog. Polym. Sci.* **2007**, *32*, 762; c) T. Ware, A. R. Jennings, Z. S. Bassampour, D. Simon, D. Y. Son, W. Voit, *RSC Adv.* **2014**, *4*, 39991.
[4] D. E. Discher, A. Eisenberg, *Science* **2002**, *297*, 967.
[5] a) O. Koshkina, C. Bantz, C. Wuerth, T. Lang, U. Resch-Genger, M. Maskos, in *Advanced Polymers in Medicine* (Eds: A. Lendlein, D. W. Grijpma), WILEY-VCH Verlag GmbH & Co. KGaA, Weinheim **2011**, p. 141; b) A. F. Thünemann, R. Bienert, D. Appelhans, B. Voit, *Macromol. Chem. Phys.* **2012**, *213*, 2362; c) O. Koshkina, T. Lang, R. Thiermann, D. Docter, R. H. Stauber, C. Secker, H. Schlaad, S. Weidner, B. Mohr, M. Maskos, A. Bertin, *Langmuir* **2015**, *31*, 8873.
[6] J. Wu, Z.-G. Su, G.-H. Ma, *Int. J. Pharm.* **2006**, *315*, 1.
[7] S. E. Stiriba, H. Frey, R. Haag, *Angew. Chem., Int. Ed.* **2002**, *41*, 1329.
[8] a) W. Sokolowski, A. Metcalfe, S. Hayashi, L. Yahia, J. Raymond, *Biomed. Mater.* **2007**, *2*, 23; b) W. Small, P. Singhal, T. S. Wilson, D. J. Maitland, *J. Mater. Chem.* **2010**, *20*, 3356; c) M. C. Serrano, G. A. Ameer, *Macromol. Biosci.* **2012**, *12*, 1156; d) P. Singhal, W. Small, E. Cosgriff-Hernandez, D. J. Maitland, T. S. Wilson, *Acta Biomater.* **2014**, *10*, 67.
[9] a) C. Liu, H. Qin, P. T. Mather, *J. Mater. Chem.* **2007**, *17*, 1543; b) D. Ratna, J. Karger-Kocsis, *J. Mater. Sci.* **2008**, *43*, 254; c) A. Lendlein, *Shape-Memory Polymers*, Springer, Berlin Heidelberg **2010**, p. 209; d) T. Pretsch, *Polymers* **2010**, *2*, 120; e) M. D. Hager, S. Bode, C. Weber, U. S. Schubert, *Prog. Polym. Sci.* **2015**, *49–50*, 3; f) Q. Zhao, H. J. Qi, T. Xie, *Prog. Polym. Sci.* **2015**, *49–50*, 79.
[10] a) M. C. Chen, H. W. Tsai, Y. Chang, W. Y. Lai, F. L. Mi, C. T. Liu, H. S. Wong, H. W. Sung, *Biomacromolecules* **2007**, *8*, 2774; b) W. Small, P. R. Buckley, T. S. Wilson, W. J. Benett, J. Hartman, D. Saloner, D. J. Maitland, *IEEE Trans. Biomed. Eng.* **2007**, *54*, 1157; c) L. Xue, S. Dai, Z. Li, *Biomaterials* **2010**, *31*, 8132.
[11] A. Lendlein, R. Langer, *Science* **2002**, *296*, 1673.
[12] K. Kratz, U. Voigt, A. Lendlein, *Adv. Funct. Mater.* **2012**, *22*, 3057.
[13] a) T. Ware, D. Simon, R. L. Rennaker II, W. Voit, *Polym. Rev.* **2013**, *53*, 108; b) T. Ware, D. Simon, C. Liu, T. Musa, S. Vasudevan, A. Sloan, E. W. Keefer, R. L. Rennaker II, W. Voit, *J. Biomed. Mater. Res., Part B* **2014**, *102*, 1.
[14] a) T. Ware, D. Simon, K. Hearon, C. Liu, S. Shah, J. Reeder, N. Khodaparast, M. P. Kilgard, D. J. Maitland, R. L. Rennaker, II, W. E. Voit, *Macromol. Mater. Eng.* **2012**, *297*, 1193; b) T. Ware, D. Simon, D. E. Arreaga-Salas, J. Reeder, R. Rennaker, E. W. Keefer, W. Voit, *Adv. Funct. Mater.* **2012**, *22*, 3470; c) T. Ware, D. Simon, K. Hearon, T. H. Kang, D. J. Maitland, W. Voit, *Macromol. Biosci.* **2013**, *13*, 1640.
[15] a) J. P. Harris, J. R. Capadona, R. H. Miller, B. C. Healy, K. Shanmuganathan, S. J. Rowan, C. Weder, D. J. Tyler, *J. Neural Eng.* **2011**, *8*, 066011; b) J. P. Harris, A. E. Hess, S. J. Rowan, C. Weder, C. A. Zorman, D. J. Tyler, J. R. Capadona, *J. Neural Eng.* **2011**, *8*, 046010; c) A. E. Hess, J. R. Capadona, K. Shanmuganathan, L. Hsu, S. J. Rowan, C. Weder, D. J. Tyler, C. A. Zorman, *J. Micromech. Microeng.* **2011**, *21*, 054009; d) J. R. Capadona, D. J. Tyler, C. A. Zorman, S. J. Rowan, C. Weder, *MRS Bull.* **2012**, *37*, 581; e) J. K. Nguyen, D. J. Park, J. L. Skousen, A. E. Hess-Dunning, D. J. Tyler, S. J. Rowan, C. Weder, J. R. Capadona, *J. Neural Eng.* **2014**, *11*, 056014; f) M. Jorfi, J. L. Skousen, C. Weder, J. R. Capadona, *J. Neural Eng.* **2015**, *12*, 011001; g) J. K. Nguyen, M. Jorfi, K. L. Buchanan, D. J. Park, E. J. Foster, D. J. Tyler, S. J. Rowan, C. Weder, J. R. Capadona, *Acta Biomater.* **2016**, *29*, 81.
[16] P. D. Nair, *J. Biomater. Appl.* **1995**, *10*, 121.
[17] FDA, "Updated 510(k) sterility review guidance K90-1; Guidence for industry and FDA", US Department of Health and Human Services FDA, Center for Devices and Radiological Health, **2016**.
[18] a) J. C. Kelsey, *J. Clin. Pathol.* **1961**, *14*, 59; b) I. P. Matthews, C. Gibson, A. H. Samuel, *Clin. Mater.* **1994**, *15*, 191.
[19] a) L. De Nardo, R. Alberti, A. Cigada, L. Yahia, M. C. Tanzi, S. Farè, *Acta Biomater.* **2009**, *5*, 1508; b) L. De Nardo,

M. Moscatelli, F. Silvi, M. C. Tanzi, L. H. Yahia, S. Farè, *J. Mater. Sci.: Mater. Med.* **2010**, *21*, 2067; c) L. De Nardo, S. Bertoldi, M. C. Tanzi, H. J. Haugen, S. Farè, *Smart Mater. Struct.* **2011**, *20*, 035004; d) S. Todros, C. Venturato, A. N. Natali, G. Pace, V. Di Noto, *J. Polym. Sci., Part B: Polym. Phys.* **2014**, *52*, 1337; e) T. A. M. Valente, D. M. Silva, P. S. Gomes, M. H. Fernandes, J. D. Santos, V. Sencadas, *ACS Appl. Mater. Interfaces* **2016**, *8*, 3241; f) C. Yavuz, S. N. B. Oliaei, B. Cetin, O. Yesil-Celiktas, *J. Supercrit. Fluids* **2016**, *107*, 114; g) L. De Nardo, S. Bertoldi, A. Cigada, M. C. Tanzi, H. J. Haugen, S. Farè, *J. Appl. Biomater. Funct. Mater.* **2012**, *10*, 119; h) M. C. Tanzi, L. De Nardo, S. Bertoldi, S. Farè, in *Shape Memory Polymers for Biomedical Applications* (Ed: L. Yahia), Elsevier Ltd, Cambridge, UK **2015**, p. 133; i) S. Bertoldi, S. Farè, H. J. Haugen, M. C. Tanzi, *J. Mater. Sci.: Mater. Med.* **2015**, *26*, 1.

[20] C. M. Yakacki, M. B. Lyons, B. Rech, K. Gall, R. Shandas, *Biomed. Mater.* **2008**, *3*, 015010.

[21] Y. Wong, J. Kong, L. K. Widjaja, S. S. Venkatraman, *Sci. China: Chem.* **2014**, *57*, 476.

[22] a) C. E. Hoyle, T. Y. Lee, T. Roper, *J. Polym. Sci., Part A: Polym. Chem.* **2004**, *42*, 5301; b) C. E. Hoyle, C. N. Bowman, *Angew. Chem., Int. Ed.* **2010**, *49*, 1540.

[23] a) H. Cao, E. Currie, M. Tilley, Y. C. Jean, in *Photoinitiated Polymerization*, American Chemical Society, Washington, DC **2003**, p. 152; b) J. A. Arceneaux, *UV + EB Technol. – Print. Packag. Innovations* **2015**, *1*, 48.

[24] N. B. Cramer, C. N. Bowman, *J. Polym. Sci., Part A: Polym. Chem.* **2001**, *39*, 3311.

[25] a) H. Drnovská, L. Lapčík, V. Buršíková, J. Zemek, A. M. Barros-Timmons, *Colloid Polym. Sci.* **2003**, *281*, 1025; b) C. Corbella, S. Grosse-Kreul, A. von Keudell, *Plasma Processes Polym.* **2015**, *12*, 564; c) M. Vishnuvarthanan, N. Rajeswari, *Innovative Food Sci. Emerging Technol.* **2015**, *30*, 119.

[26] F. D. A. United States Department of Health and Human Services – Office of Regulatory Affairs (ORA), "Guidance for Industry Pyrogen and Endotoxins Testing: Questions and Answers," United States Department of Health and Human Services – Office of Regulatory Affairs (ORA), Food and Drug Administration, **2012**.

[27] a) P. J. Kropp, G. E. Fryxell, M. W. Tubergen, M. W. Hager, G. D. Harris, T. P. McDermott, R. Tornero-Velez, *J. Am. Chem. Soc.* **1991**, *113*, 7300; b) P. Filipiak, G. L. Hug, B. Marciniak, *J. Photochem. Photobiol. A: Chem.* **2006**, *177*, 295.

[28] M. Ravikumar, D. J. Hageman, W. H. Tomaszewski, G. M. Chandra, J. L. Skousen, J. R. Capadona, *J. Mater. Chem. B, Mater. Biol. Med.* **2014**, *2*, 2517.

[29] H. Levine, L. Slade, *Water Science Reviews 3*, Cambridge University Press, Cambridge, UK **1988**.